6.11

Sediment Diagenesis and Benthic Flux

S. Emerson and J. Hedges

University of Washington, Seattle, WA, USA

6.11.1 INTRODUCTION

Chemical reactions in marine sediments and the resulting fluxes across the sediment–water interface influence the global carbon cycle and the pH of the sea and affect the abundance of $CaCO_3$ and opal-forming plankton in the ocean. On very long timescales these diagenetic reactions control carbon burial in sedimentary rocks and the oxygen content of the atmosphere. Sedimentary deposits that remain after diagenesis are the geochemical artifacts used for interpreting past changes in ocean circulation, biogeochemical cycles, and climate. This chapter is about the processes of diagenesis and burial of the chemical elements that make up the bulk of the particulate matter that reaches the seafloor (organic matter, $CaCO_3$, SiO_2, Fe, Mn, and aluminosilicates).

Understanding of sediment diagenesis and benthic fluxes has evolved with advances in both experimental methods and modeling. Measurements of chemical concentrations in sediments, their associated pore waters and fluxes at the sediment–water interface have been used to identify the most important reactions. Because transport in pore waters is usually by molecular diffusion, this medium is conducive to interpretation by models of heterogeneous chemical equilibrium and kinetics. Large chemical changes and manageable transport mechanisms have led to elegant models of sediment diagenesis and great advances in understanding of diagenetic processes.

We shall see, though, that the environment does not yield totally to simple models of chemical equilibrium and chemical kinetics, and laboratory determined constants often cannot explain the field observations. For example, organic matter degradation rate constants determined from modeling are so variable that there are essentially no constraints on these values from laboratory experiments. In addition, reaction rates of $CaCO_3$ and opal dissolution determined from modeling pore waters usually cannot be reproduced in laboratory experiments of these reactions. The inability to mechanistically understand reaction kinetics calculated from diagenesis models is an important uncertainty in the field today.

Processes believed to be most important in controlling the preservation of organic matter have evolved from a focus on the lability of the substrate to the protective mechanisms of mineral–organic matter interactions. The specific electron acceptor is not particularly important during very early diagenesis, but the importance of oxygen to the degradation of organic matter during later stages of diagenesis has been clarified by the study of diagenesis in turbidites deposited on the ocean floor during glacial periods.

Evolution of thinking about the importance of reactions between seawater and detrital clay minerals has come full circle since the mid-1960s. "Reverse weathering" reactions were hypothesized in very early chemical equilibrium (Sillen, 1961) and mass-balance (Mackenzie and Garrels, 1966) models of the oceans. Subsequent observations that marine clay minerals generally resemble those weathered from adjacent land and the discovery of hydrothermal circulation put these ideas on the back burner. Recent studies of silicate and aluminum diagenesis, however, have rekindled awareness of this process, and it is back in the minds of geochemists as a potentially important process for closing the marine mass balance of some elements.

6.11.2 DIAGENESIS AND PRESERVATION OF ORGANIC MATTER

Roughly 90% of the organic matter that exits the euphotic zone of the ocean is degraded in the water column. Of the ~10% of the organic carbon flux that reaches the seafloor, only about one-tenth escapes oxidation and is buried. Degradation of the organic matter that reaches the ocean sediments drives the reactions that control sediment diagenesis and benthic flux.

We begin our discussion with what we call the "pillars" of knowledge in the field—those concepts that are basic to understanding the mechanisms of organic matter diagenesis and on which future developments rested. This is followed by a description of the dominant mechanisms of organic-matter diagenesis as one progresses from oxic through the anoxic conditions. Finally, we will discuss factors controlling the reactivity of organic matter and the mechanisms of organic matter preservation.

6.11.2.1 The Pillars of Organic Matter Diagenesis

The basic concepts of organic matter diagenesis are described here as (i) the *thermodynamic* sequence of reactions of electron acceptors and their *stoichiometry*, and (ii) the *kinetics* of organic matter degradation as described by the diagenesis equations and observations of degradation rates. These ideas derived mainly from studies of ocean sediments in which pore-water transport is controlled by molecular diffusion (deepsea oxic and anoxic-SO_4 reducing), but represent the intellectual points of departure for studying near-shore systems where transport is more complicated, but where the bulk of marine organic matter is degraded.

6.11.2.1.1 Thermodynamics and sequential use of electron acceptors

The large highly structured molecules of organic matter are formed by energy from the sun and exist at atmospheric temperature and pressure in a reduced, thermodynamically unstable state. These compounds subsequently undergo reactions with oxidants to decrease the free energy of the system. The oxidants accept electrons from the organic matter during oxidation reactions (Stumm and Morgan, 1981). The electron acceptors that are in major abundance in the environment include O_2, NO_3^-, Mn(IV), Fe(III), SO_4^{2-}, and organic matter itself during fermentation (described here as methane production). These reactions are listed in the order of the free energy gained in Table 1. Half reactions for both the organic matter oxidation and the electron-acceptor reductions are represented. The changes in free energy for the reactions depend on the free energy of formation of the solids involved (organic matter, iron, and manganese oxides), and thus vary slightly among compilations in the literature. Note that the amounts of free energy gain for the whole reactions involving oxygen, nitrate, and manganese are similar. Values drop-off dramatically for iron and sulfate reactions and then again for methane production. The sequence

Table 1 The standard free energy of reaction, ΔG_r^o, for the main environmental redox reactions.

Reaction	ΔG_r^o (kJ mol^{-1}) *(half reaction)*	ΔG_r^o (kJ mol^{-1}) *(whole reaction)*
Oxidation		
$CH_2O^a + H_2O \rightarrow CO_2 + 4H^+ + 4e^-$	−27.4	
Reduction		
$4e^- + 4H^+ + O_2 \rightarrow 2H_2O$	−491.0	−518.4
$4e^- + 4.8H^+ + 0.8NO_3^- \rightarrow 0.4N_2 + 2.4H_2O$	−480.2	−507.6
$4e^- + 8H^+ + 2MnO_2(s) \rightarrow 2Mn^{2+} + 4H_2O$	−474.5	−501.9
$4e^- + 12H^+ + 2Fe_2O_3(s) \rightarrow 4Fe^{2+} + 6H_2O$	−253.2	−280.6
$4e^- + 5H^+ + \frac{1}{2}SO_4^{2-} \rightarrow \frac{1}{2}H_2S + 2H_2O$	−116.0	−143.4
$4e^- + 4H^+ + CH_2O \rightarrow CH_4 + H_2O$	−7.0	−34.4

Standard free energies of formation from Stumm and Morgan, 1981.

[a] CH_2O represents organic matter ($\Delta G_f = -129$ kJ mol^{-1}).

Table 2 Stoichiometric organic matter oxidation reactions. Redfield ratios for x, y, and z are 106, 16, 1.

Redox process	*Reaction*
Aerobic respiration	$(CH_2O)_x(NH_3)_y(H_3PO_4)_z + (x + 2y)O_2$ $\rightarrow xCO_2 + (x + y)H_2O + yHNO_3 + zH_3PO_4$
Nitrate reduction	$5(CH_2O)_x(NH_3)_y(H_3PO_4)_z + 4xNO_3^-3$ $\rightarrow xCO_2 + 3x\mathrm{H2O} + 4xHCO_3^- + 2xN_2 + 5yNH_3 + 5zH_3PO_4$
Manganese reduction	$(CH_2O)_x(NH_3)_y(H_3PO_4)_z + 2xMnO_2(s) + 3xCO_2 + xH_2O$ $\rightarrow 2xMn^{2+} + 4xHCO_3^- + yNH_3 + zH_3PO_4$
Iron reduction	$(CH_2O)_x(NH_3)_y(H_3PO_4)_z + 4xFe(OH)_3 + 3xCO_2 + xH_2O$ $\rightarrow 4xFe^{2+} + 8xHCO_3^- + 3xH_2O + yNH_3 + zH_3PO_4$
Sulfate reduction	$2(CH_2O)_x(NH_3)_y(H_3PO_4)_z + xSO_4^{2-}$ $\rightarrow xH_2S + 2xHCO_3^- + 2yNH_3 + 2zH_3PO_4$
Methane production	$(CH_2O)_x(NH_3)_y(H_3PO_4)_z$ $\rightarrow xCH_4 + xCO_2 + 2yNH_3 + 2zH_3PO_4$

Source: Tromp *et al.* (1995).

of electron acceptor use is sometimes categorized into oxic diagenesis (O_2 reduction), suboxic diagenesis (NO_3^- and Mn(IV) reduction), and anoxic diagenesis (Fe(III) and SO_4^{2-} reduction and methane formation). This terminology is not used here because the definition of suboxic is vague and ambiguous. We recommend referring to these reactions using the true meaning of the terms—oxic for O_2 reduction and anoxic for the rest (anoxic-NO_3^- reduction, anoxic-Mn(IV) reduction and so forth).

While all of these reactions are favored thermodynamically, they are almost always enzymatically catalyzed by bacteria. It has been observed from the study of pore waters in deepsea sediments (e.g., Froelich *et al.*, 1979) and anoxic basins (e.g., Reeburgh, 1980) that there is an ordered sequence of redox reactions in which the most energetically favorable reactions occur first and the active electron acceptors do not overlap significantly. Bacteria are energy opportunists. Using estimates of the stoichiometry of the diagenesis reactions (Table 2) one can sketch the order and shape of reactant profiles actually observed in sediment pore-water chemistry (Figure 1). The schematic figure shows all electron acceptors in a single sequence. This is rarely observed in the environment because regions with abundant bottom-water oxygen and moderate organic matter flux to the sediments (i.e., the deep ocean) run out of reactive organic carbon before sulfate reduction becomes important. In near-shore environments, where there is sufficient organic matter flux to the sediments to activate sulfate reduction and deplete sulfate in pore waters, zones of oxygen, nitrate, and Mn(IV) reduction are very thin or obscured by benthic animal irrigation and bioturbation.

Recent global models of the importance of the different electron acceptors (Figure 2; Archer *et al.*, 2002) indicate that oxic respiration accounts for ~95% of the organic matter oxidation below 1,000 m in the ocean. However, between 80% and 90% of organic matter is buried in sediments above 1,000 m in river deltas and on continental margins (Archer *et al.*, 2002; Hedges and Keil, 1995). Anoxic diagenesis is more important in these regions, and when they are included, oxic diagenesis accounts for ~70% of the total organic matter oxidation in marine sediments.

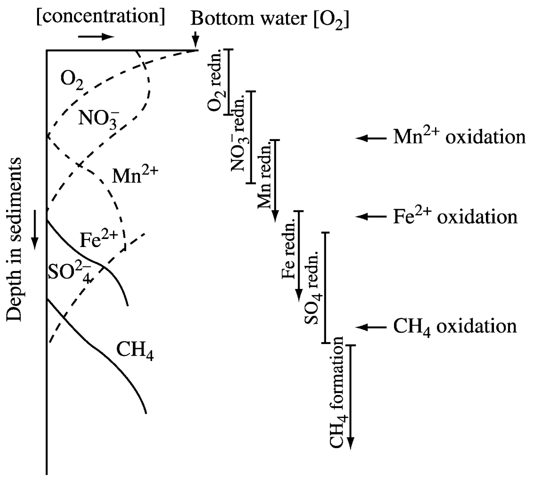

Figure 1 A schematic representation of the pore-water result of organic matter degradation by sequential use of electron acceptors.

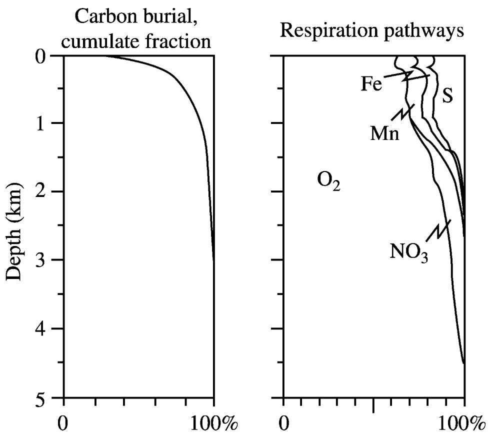

Figure 2 The cumulative fraction of carbon burial and the respiration pathways as a function of depth in the ocean derived from the global diagenesis model of Archer *et al.* (2002) (after Archer *et al.*, 2002).

6.11.2.1.2 Kinetics of organic matter degradation

The second "pillar" in our understanding of organic matter diagenesis and benthic flux consists of advances in quantifying the rates of organic matter degradation and burial. The kinetics of organic matter degradation have been determined by modeling environmental pore-water data and in laboratory studies. Most models of organic matter degradation have derived in some way from the early studies by Berner on this subject (e.g., Berner, 1980). In its simplest form, one-dimensional diagenesis, the change in organic carbon concentration (C_s, g C g_s^{-1}; s = dry sediment) with respect to time and depth is

$$\frac{\partial}{\partial t}(\rho(1-\phi)C_s) = \frac{\partial}{\partial z}\left(D_b\frac{\partial(\rho(1-\phi)C_s)}{\partial z}\right) - \frac{\partial}{\partial z}(\omega\rho(1-\phi)C_s) + MR \qquad (1)$$

where z is depth below the sediment–water interface (positive downward), ϕ is porosity ($\mathrm{cm}_{\mathrm{pw}}^3/\mathrm{cm}_{\mathrm{b}}^3$; where pw is pore water and b is bulk), ρ is the dry sediment density (g cm_s^{-3}), M (g mol^{-1}) is the molecular weight of carbon, D_b ($\mathrm{cm}_b^2\,\mathrm{s}^{-1}$; s = second) is the sediment bioturbation rate, ω is the sedimentation rate ($\mathrm{cm}_b\,\mathrm{s}^{-1}$), and R ($\mathrm{mol\,cm}_b^{-3}\,\mathrm{s}^{-1}$) is the reaction term. Organic matter degradation is usually considered to be first order with respect to substrate concentration so

$$R = kC_s(1-\phi)\rho/M \qquad (2)$$

where k is the first-order degradation rate constant. Probably the largest simplification here is that stirring of sediments by animals is modeled as a random process analogous to molecular diffusion. This is a gross simplification to reality. It has been shown that different tracers of bioturbation yield different results and animal activity varies with organic matter flux to the sediment–water interface (Aller, 1982; Smith *et al.*, 1993; Smith and Rabouille, 2002).

The reaction–diffusion equation for the concentration of the pore-water constituent, C_d ($\mathrm{mol\,cm}_{\mathrm{pw}}^{-3}$) is

$$\frac{\partial}{\partial t}(\phi C_d) = \frac{\partial}{\partial z}\left(D\frac{\partial(\phi)C_d}{\partial z}\right) - \frac{\partial}{\partial z}(v\phi C_d) + \gamma R \qquad (3)$$

where D now represents the molecular diffusion coefficient and v (cm s^{-1}) is the velocity of water (which is only the same as the sediment burial, ω, when porosity is constant and there is no outside-induced flow; Imboden (1975)) and γ is a stoichiometric ratio of the pore-water element to organic carbon. At steady state with respect to compaction and the boundary conditions, the left side of Equation (3) is zero and v and ω are equal below the depth of porosity change. A very detailed treatment of many different cases is presented in Berner (1980) and Boudreau (1997).

After application of the diagenesis equations to a variety of marine environments, it became clear that the organic matter degradation rate constant, k, derived to fit the pore water and sediment profiles, was highly variable. The organic fraction of such sediments is thus often modeled as a mixture of a small number of discrete components (G_i), each of which has a finite initial amount and first-order decay constant (e.g., Jørgensen, 1979; Westrich and Berner, 1984). An alternative to such discrete models is to treat sedimentary organic matter as containing either one component whose reactivity decreases continuously over time (Middelburg, 1989), or as a continuum of multiple components whose distribution changes over time (Boudreau and Ruddick, 1991). All these discrete and continuum models capture the fundamental feature that bulk organic matter breaks down at an increasingly slower rate as it degrades.

A consequence of this broad continuum in reactivity is that sedimentary organic matter can be observed to degrade on essentially all timescales of observation. Although slightly different degradation rates may be measured for various components of a sedimentary mixture, such as different elements or biochemicals, the range of absolute values of the measured rate constants closely correspond to the time span represented by the experimental data (Emerson and Hedges, 1988; Middelburg, 1989). This direct correspondence in observation period (in units of time) and measured degradation rate constant (in units of inverse time) extends over eight orders of magnitude from days to millions of years (Figure 3). A result of the high order kinetics is that components of sedimentary mixtures that react more slowly will become a much greater fraction of unreacted material while the reaction rate constant (the curvature) is mainly described by the more labile components.

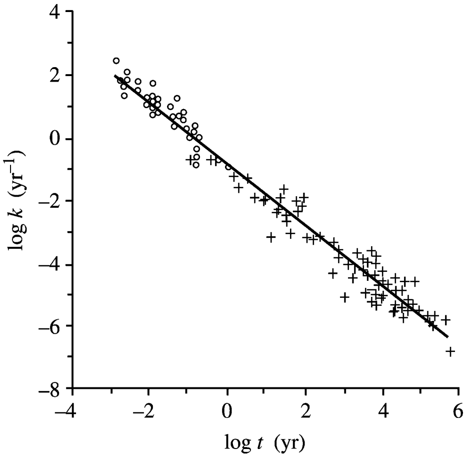

Figure 3 The rate constant, *k*, for organic matter degradation versus the age of the organic matter undergoing degradation determined from models of pore waters and laboratory experiments (after Middelburg, 1989) (reproduced by permission of Elsevier from *Geochim. Cosmochim. Acta* **1989**, *53*, 1577–1581). Circles are data from laboratory experiments. Crosses were determined by models of organic carbon versus depth. The line is drawn through the points.

6.11.2.2 Organic Matter Diagenesis Down the Redox Progression

6.11.2.2.1 O_2, NO_3^-, and Mn(IV) diagenesis

The relationships among the flux of organic carbon to the sediment–water interface and its diagenesis and burial in deep-ocean sediments where oxygen is the primary electron acceptor is depicted in Figure 4(a) (Emerson *et al*., 1985). In this case one identifies two cases—one is carbon limited, where measurable oxygen persists in the pore waters at a depth of about one meter and one that is oxygen limited in which oxygen goes to zero at some depth within the bioturbated zone. Emerson *et al.* (1985) demonstrated that the measurements of carbon flux in near-bottom sediment traps was consistent with pore-water metabolite fluxes and the organic carbon content of the sediments assuming reasonable bioturbation rates at three sites in the eastern and central equatorial Pacific. Examples of carbon limited diagenesis (Figure 4(b)) are in locations of relatively low particulate organic carbon flux to the sediments such as the pelagic North Pacific and Atlantic and some carbonate-rich locations in the western equatorial Pacific (Grundmanis and Murray, 1982; Wilson *et al*., 1985; Murray and Kuivila, 1990; Rutgers van der Loeff, 1990). Diagenesis in most of the rest of marine sediments >1,000 m is oxygen limited. Emerson *et al.* (1985) used an oxygen-only model for the oxygen-limited case to suggest that the two dominant factors controlling the organic carbon content in deep-ocean sediments are the carbon rain rate to the sediments and the concentration of oxygen in the bottom waters. This suggestion was challenged by others who believed anoxic diagenesis is efficient enough to consume most of the carbon left after the pore waters become oxygen depleted (e.g., Pedersen and Calvert, 1990; Calvert and Pedersen, 1992). We return to this subject in Section 6.11.2.4.

Nitrate plays an important role as a tracer of both oxic and anoxic (NO_3^--reducing) diagenesis because it is both produced and consumed during these processes (Table 2). Bender *et al.* (1977) and Froelich *et al.* (1979) used these relationships to infer the depth of the zone of oxic diagenesis. Middelburg *et al.* (1996) estimated that the contribution of denitrification to total sediment organic matter degradation is 7–11%, and that the global denitrification rate in sediments is ~18 × 10^{12} mol N yr^{-1}. The latter value is at least a factor of 2 greater than water-column denitrification, indicating the importance of marine sediments as sink for fixed nitrogen.

Manganese and iron oxides are two solid phase electron acceptors that play important roles in organic matter degradation. Their effect is limited by the liability of the solid to

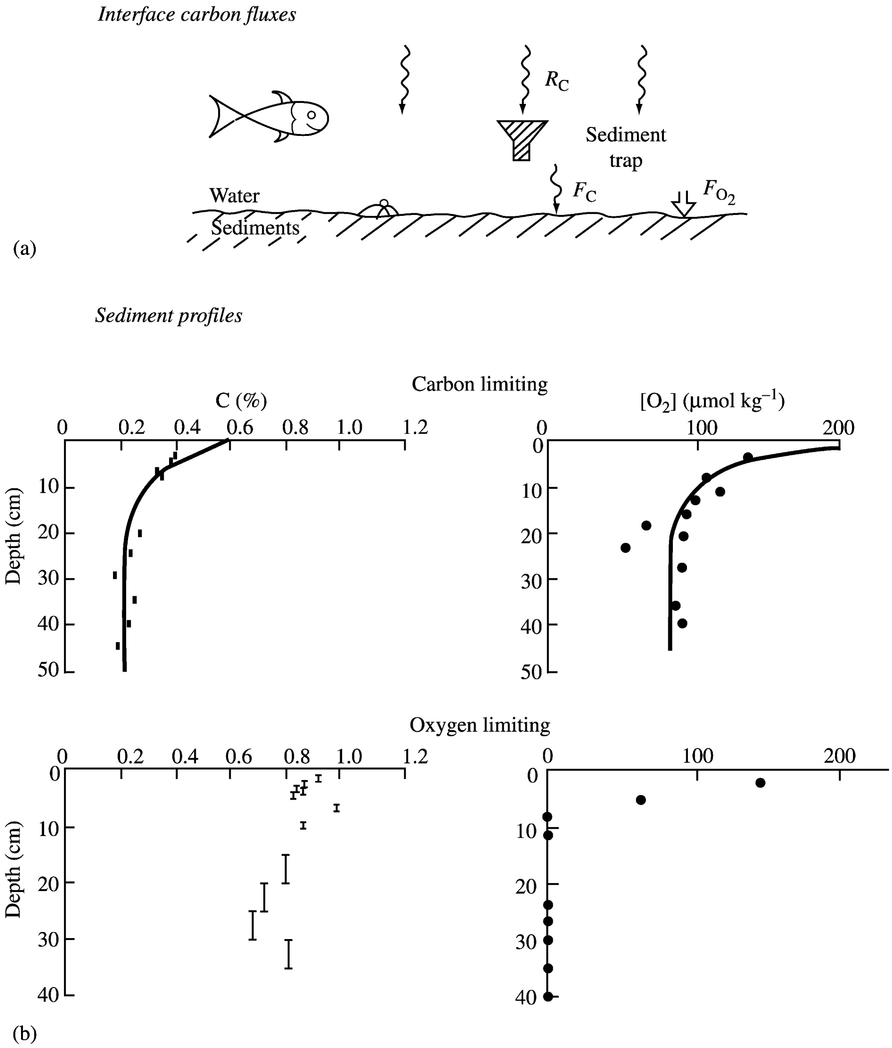

Figure 4 (a) A schematic representation of the fluxes of organic matter and oxygen at the sediment–water interface of the deep sea. R_C is the rain rate of particulate organic carbon and F_C and F_{O_2} are the fluxes of organic carbon and oxygen at the sediment–water interface (source Emerson *et al.*, 1985). (b) Data indicating the carbon- and oxygen-limiting cases. The carbon-limiting case is redrawn from Grundmanis and Murray (1982), and the oxygen-limited data are from Murray and Kuivila (1990).

dissolution, which is not easily quantified experimentally (e.g., Raiswell *et al.*, 1994), creating another unknown in models of these reactions. Manganese is reduced nearly simultaneously with nitrate, which is consistent with the comparable amounts of free energy available (Table 1). The produced Mn^{2+} is then either transported to the overlying water or reoxidized by oxygen. This relocation process is ubiquitous in oxygen-limited areas of marine sediments and creates manganese enrichment in surface sediments of the deep ocean. Although manganese cycling has the most important impact on organic matter diagenesis in near-shore sediments (Figures 2 and 5), it also has been shown to play an extremely important role in deepsea locations of relatively high organic carbon rain and labile, hydrothermally derived manganese. Aller (1990) demonstrated that nearly all organic matter degradation in sediments of the Panama Basin (eastern equatorial Pacific) is oxidized by the reduction of Mn(IV). The flux of oxygen determined by microelectrode O_2 profiles nearly balanced the flux of Mn(II) from below. The net redox reaction in this location is dominated by organic matter oxidation and O_2 reduction, but with the intermediate oxidation and reduction of manganese. The unusual availability of oxidized Mn(IV) (~3 wt.%) creates a very different redox environment than in deepsea locations where solid manganese concentrations are near shale values (~0.08 wt.%).

Sediment diagenesis reactions cause sources and sinks that are of global importance to the geochemical mass balance of manganese and some other metals sensitive to redox changes.

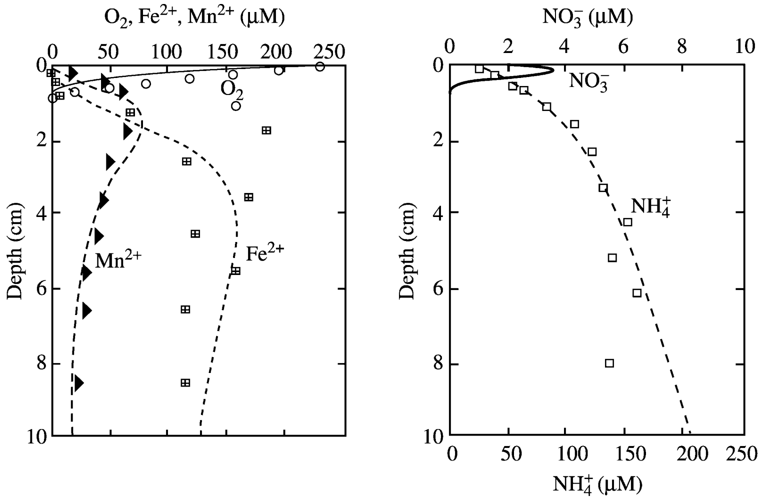

Figure 5 Pore-water profiles of O_2, Fe(II), Mn(II), NO_3^-, and NH_4^+ from sediments of the near-shore waters of Denmark. Symbols represent data from Canfield *et al.* (1993) and lines are model results from Wang and Van Cappellen (1996) (after Wang and Van Cappellen, 1996) (reproduced by permission of Elsevier from *Geochim. Cosmochim. Acta* **1996**, *60*, 2993–3014).

Morford and Emerson (1999) were able to quantify this effect using experimental evidence that indicated manganese and vanadium are remobilized to the ocean when oxygen penetrates pore waters 1 cm or less. Other redox-sensitive elements (rhenium, cadmium, and uranium) are taken up in the sediments under these redox conditions. They then applied the oxygen- and carbon-only models discussed in Section 6.11.2.2 and distributions of bottom-water O_2 and particulate organic carbon rain to the sediments below 1,000 m (Jahnke, 1996) to determine that the global extent of this redox condition is ~3% of the sediments. For manganese, vanadium, and rhenium the fluxes from and to the more reducing areas are very large even though the calculation must be considered a minimum because the sediments shallower than 1,000 m were not considered. For example, the manganese flux from the reducing sediments on the ocean margins is 1.4–2.6 times that from rivers indicating a massive redistribution of this element within the ocean basins.

6.11.2.2.2 Fe, SO_4^{2-} reduction, and CH_4 production

As one approaches continents from the deep ocean, overlying productivity becomes greater and the water depth shoals so that particles are degraded less while sinking. Both factors increase the particulate organic matter flux to the sediment–water interface. This creates more extensive anoxia in the sediments, which is sometimes compounded on continental slopes by low bottom-water oxygen conditions. A natural result of the greater supply of organic matter to the sediments is that benthic animals become bigger and more diverse. The consequence to organic matter diagenesis is that bioturbation is deeper and more intense and that animal irrigation activities are rapid enough to compete with molecular diffusion as the mechanism of pore-water transport.

The relative roles of diffusion and animal-induced advection across the sediment–water interface has been quantified by comparing oxygen fluxes determined by benthic lander measurements with those calculated from pore-water micro-electrode oxygen profiles (Figure 6; Archer and Devol, 1992). As one progresses up the continental slope and onto the shelf of the northwest US the fluxes determined by these two methods diverge. Those determined from the benthic lander become greater at depths <~100 m indicating the local importance of animal irrigation activity. This process complicates the diagenetic redox balance in coastal marine sediments, where 80–90% of marine organic matter is buried, because it is much more difficult to generalize on the mechanism and magnitude of animal irrigation than molecular diffusion.

Aller (1984) created a mechanistic model for the multi-dimensional transport of dissolved pore-water species by animals. He observed that ammonia profiles caused by sulfate reduction in the top-ten-centimeter layer of Long Island Sound sediments could not be interpreted by one-dimensional diffusion (Equation (3)). The multi-dimensional effects of irrigation were reproduced mathematically by characterizing the top layer of

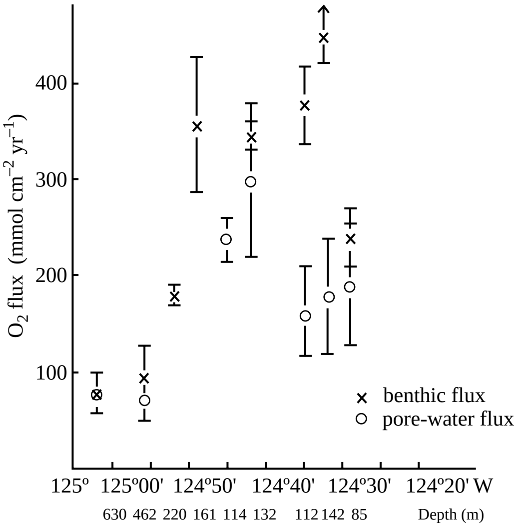

Figure 6 Oxygen fluxes determined from benthic lander measurements (×) and calculated from microelectrode oxygen gradients measured in the top few centimeters of pore waters (○) as a function of latitude and depth on the northwest US continental margin. Error bars are the standard deviation of replicate measurements (after Archer and Devol, 1992).

the sediments as a system of closely packed hollow cylinders. Integration of the equations for radial diffusion using geometries for the inner- and outer-cylinder radii determined from field measurements resulted in pore-water ammonia profiles that reproduced observations. Many subsequent "nonlocal" models of irrigation (Christensen *et al.*, 1984; Emerson *et al.*, 1984; Boudreau, 1984) have been able to reproduce the essential characteristics of animal irrigation without the complexity or elegance of the multidimensional model, but require a nonlocal transport rate. This approach has been adopted in most of the general models of sediment diagenesis (e.g., Wang and Van Cappellen, 1996; Archer *et al.*, 2002).

Wang and Van Cappellen (1996) demonstrated the intense interplay between the redox coupling of iron and manganese and transport by animal activity in the sediments of the eastern Skagerrak between Denmark and Norway (Canfield *et al.*, 1993). Sediment pore-water profiles from this area (Figure 5) indicate that most Mn(IV) reduction is coupled to oxidation of Fe(II) which was formed during organic matter and H_2S oxidation. Again the manganese and iron redox cycles shuttle electrons between more oxidized and reduced species. Adsorption of the reduced dissolved form of these metals to sediment surfaces plays an important role in their reactivity and transport by bioturbation and irrigation back to the surface sediments where they are reoxidized or transported to the overlying waters. In general, most of the iron redox cycling occurs within the sediments because of the relatively rapid oxidation kinetics of Fe(II) while some of the recycled Mn(II) escapes to the bottom waters because it is reduced nearer the sediment–water interface and has slower oxidation kinetics.

Shallow environments at the mouths of tropical rivers are the deposition sites of ~60% of the sediment delivered to the ocean (Nittrouer *et al.*, 1991). In some of these locations seasonal resuspension of the sediments occurs to a depth of 1–2 m to form fluid muds. This setting creates a very different type of sediment diagenesis that is characterized by intense iron and manganese reactions but little sulfate reduction or methane formation. Because organic matter is abundant at these shallow river-mouth locations, oxygen is depleted relatively rapidly after deposition. Abundant oxidized iron and manganese in these highly weathered sediments are reduced, creating massive, time-dependent increases in pore-water iron and manganese (Aller *et al.*, 1986). The period of diagenesis; however, is not long enough between resuspension events for sulfate reduction to become established. This situation is one of extreme non-steady-state diagenesis in which pore-water transport is dominated by physical mechanisms rather than animal irrigation or molecular diffusion.

In near-shore regions where organic matter flux to the sediments is high or bottom-water oxygen concentrations are low and horizontal sediment transport does not dominate, sulfate reduction and subsequent methane formation are important processes (Martins *et al.*, 1980; Reeburgh, 1980). Some of the earliest studies of steady-state diagenesis were applied to measurements of pore waters in Long Island Sound and Santa Barbara Basin sediments to interpret organic matter degradation by anoxic, SO_4^{2-}-reduction reactions (Berner, 1974). Early measurements of SO_4^{2-} and CH_4 in marine pore waters indicated that methane appears only after most of the SO_4^{2-} has been reduced (Figure 7), creating profiles that do not overlap significantly much like those of O_2 and Mn(IV) and Fe(II) and NO_3^-. Locations of methane formation are restricted in the marine environment because of the high sulfate concentrations in seawater. This is not true in freshwater systems where abundant CH_4 production occurs because organic matter is abundant and SO_4^{2-} concentrations are low.

Reeburgh (1980) suggested that the pore-water distributions of SO_4^{2-} and CH_4 indicate that CH_4 is being oxidized anaerobically with SO_4 being the electron acceptor. This suggestion, which is virtually unavoidable based on the metabolite distributions and interpretation by diffusion equations (see also Murray *et al.*, 1978), was not

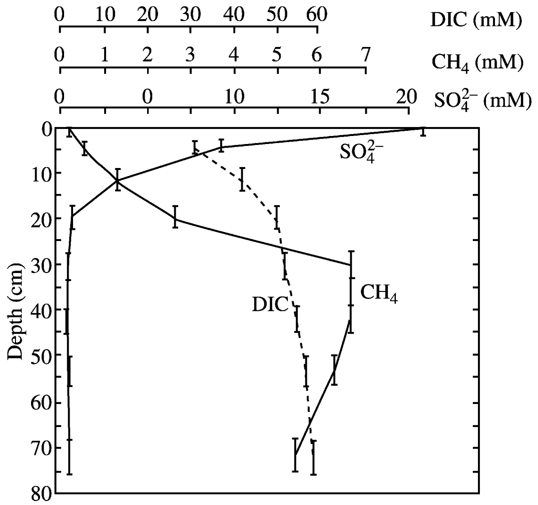

Figure 7 Pore-water profiles of SO_4^{2-}, CH_4, and DIC from the sediments of Scan Bay Alaska an anoxic fjord (after Reeburgh, 1980) (reproduced by permission of Elsevier from *Earth Planet. Sci.* **1980**, *47*, 345–352).

accepted initially by many microbiologists because it has been difficult to culture the SO_4^{2-} reducing/CH_4 oxidizing bacteria.

6.11.2.3 Benthic Respiration

Jahnke (1996) extrapolated available benthic-flux measurements from landers and pore-water determinations into a global map of benthic oxygen flux for sediments deeper than 1,000 m. When compared with global primary production rates and sediment-trap particle fluxes, these data indicate that ~1% of the primary production reaches deep-sea sediments and is oxidized there (Table 3). Also ~45% of respiration in the ocean below 1,000 m occurs within sediments.

Because particulate carbon export from surface waters is seasonal, and it is known that the majority of the particle flux is by large rapidly falling particles, one might expect that the benthic flux would also vary seasonally. This was shown to be true in the North Pacific by a series of benthic respiration deployments (Smith and Baldwin, 1984), but not in the North Atlantic near Bermuda (Sayles *et al.*, 1994). The reason for these differences is not presently understood.

The isotopes of oxygen and nitrogen gas should ideally be tracers of the relative amount of O_2 and NO_3^- reduction that takes place in the water column and sediments because the fractionation factor in a diffusive medium is theoretically equal to the square root of that in a completely open system (Bender, 1990). Brandes and Devol (1997) tested this model by measuring the fractionation of oxygen and nitrogen gas in sediments using a benthic lander. They found that the situation was more complicated than that predicted from the diffusion model. The observed fractionation factors for O_2 and NO_3^- reduction in sediments were much less than the square root of the open-system isotope fractionation factor. The most logical explanation is that both oxygen reduction and denitrification take place in sediment microenvironments where most of the O_2 and NO_3^- are consumed before they have time to communicate with the overlying waters. While there have been only a few benthic-flux isotope fractionation studies, it is clear that broad generalizations about the distribution of respiration between the water column and the sediments is not possible based on isotope measurements until the isotope fractionation in sediments is better understood. This caveat should hold for all isotope systems undergoing diagenesis in marine sediments.

Table 3 Comparison of benthic oxygen fluxes at the sediment–water interface and primary production (PP) in the ocean's euphotic zone.

Latitude	*PP* (10^{14} mol C yr^{-1})	*Benthic flux* (10^{14} mol C yr^{-1})	*% of PP*
10° N–10° S	2.08	0.020	1.0
11° N–37° N	2.67	0.026	1.0
38° N–50° N	0.83	0.008	1.0
50° N–60° N	0.41	0.005	1.1

Source: Jahnke (1996).

6.11.2.4 Factors Controlling Organic Matter Degradation

There are many factors that contribute to the seemingly universal slowing of organic matter decomposition with time. One of these is that the physical form and distribution of organic matter within sediments is not uniform. A second is that the rate and extent of organic matter degradation can vary with the different inorganic electron acceptors available at different stages of degradation. Finally, the structural features of the residual organic matter mixture may vary over time as more readily utilized components are oxidized or converted into less-reactive products.

6.11.2.4.1 Mineral association

It has long been recognized that organic matter tends to concentrate in fine-grained continental margin sediments, as opposed to coarser silts and sands (Premuzic *et al.*, 1982). Since the early 1990s, it has become clear that organic matter and fine-grained minerals in marine sediments are physically associated. One line of evidence is that only a small fraction (~10%) of the bulk organic matter in unconsolidated marine sediments can be separated as discrete particles by flotation in heavy liquids or hydrodynamic sorting (Mayer, 1994a,b; Keil *et al.*, 1994a). In addition, the concentrations of organic carbon in bulk sediments (Suess, 1973; Mayer, 1994a; Ransom *et al.*, 1998) and their size fractions (Keil *et al.*, 1994a; Bergamaschi *et al.*, 1997) increase directly with external mineral surface area as measured by N_2 adsorption (Figure 8).

Most sediments collected under oxic waters along continental margins exhibit organic carbon (OC) concentrations ~0.5–1.0 mg OC m^{-2} (e.g., Figure 8), a "loading" that is similar to that expected for a single layer of protein spread uniformly across the surfaces of mineral grains. Such organic matter concentrations were initially referred to as being "monolayer-equivalent" a term that was introduced with the caveat that the actual distribution pattern of organic matter over mineral-grain surfaces was then unknown (Mayer, 1994a). The notion that organic matter might be spread one-molecule deep on essentially all mineral grains implies sorption of previously dissolved organic substances that are physically shielded on the mineral surface from direct degradation by bacteria and their exoenzymes. Evidence in support of the protective function came from the demonstration that over 75% of dissolved organic matter desorbed from sedimentary minerals deposited for hundreds of years could be respired within five days once removed from this matrix (Keil *et al.*, 1994b).

Although the concept that sedimentary organic matter is strongly associated with mineral surfaces has stood the test of time, the monolayer-equivalent hypothesis has not. Transmission electron micrographs of organic matter in continental margin sediments indicate that most organic matter is discontinuously distributed in discrete "blebs," mucus networks and smears that are associated with domain junctions in clay-rich flocks (Ransom *et al.*, 1997). Mayer (1999) deduced from the energetics of gas adsorption onto minerals from continental-margin sediments that generally less than 15% of the surfaces of typical sedimentary minerals are coated with organic matter.

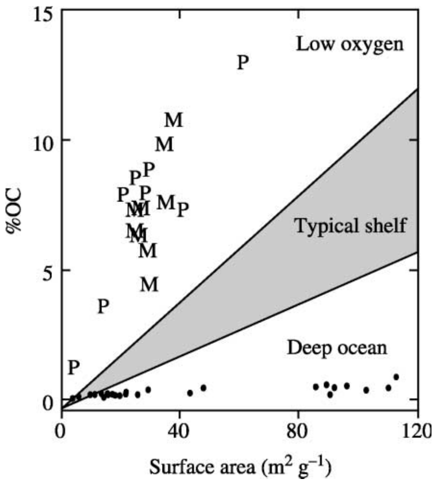

Figure 8 Weight percentages of organic carbon (%OC) plotted versus mineral surface area for surficial sediments from a range of depositional regimes. M and P represent data for samples from the Mexican and Peruvian margins, respectively (source Hedges and Keil, 1995).

Physical protection is insufficient alone to explain the distribution of organic matter in marine sediments. For example, marine sediments deposited under bottom waters with little or no dissolved O_2 usually have surface-normalized organic carbon concentrations substantially greater than 0.5–1.0 mg OC m^{-2}, whereas fine-grained deepsea clays typically contain a tenth or less of the organic concentration exhibited by continental-margin sediments of equivalent surface area (Figure 8). In particular, additional processes must account for that fact that open-ocean sediments that cover ~80% of total seafloor account for less than 5% of global organic carbon burial (Berner, 1989; Hedges and Keil, 1995).

6.11.2.4.2 The importance of oxygen

A commonly made assumption in descriptions of sedimentary diagenesis is that degradation rate and extent are largely controlled by the "quality" of available organic substrate(s), as opposed to the relative supply of different electron acceptors (Berner, 1980). This perspective is supported by a variety of field and laboratory studies (Calvert and Pedersen, 1992). In particular, freshly dissolved organic substrates (Lee, 1992; Kristensen and Holmer, 2001) and polysaccharide- and protein-rich materials (Westrich and Berner, 1984) are often degraded at similar rates in the presence or absence of molecular oxygen. However, some laboratory experiments show much slower and less efficient anoxic degradation of aged organic matter (Kristensen and Holmer, 2001) and carbon-rich substrates such as lipids (Atlas *et al.*, 1981) and pigments (Sun *et al.*, 1993a,b). Harvey *et al.* (1995) observed that the total carbon, total nitrogen, protein, lipid, and carbohydrate fractions of a diatom and coccolith were all more rapidly degraded in oxic versus anoxic laboratory incubations. Lignin, a biomacromolecule that is carbon-rich, insoluble in water and difficult to hydrolyze, is very sparingly degraded in the absence of O_2 (Benner *et al.*, 1984; Hedges *et al.*, 1985).

This apparent contradiction may be partially explained by selective initial use of easily degraded proteins and polysaccharides and the resulting concentration of carbon-rich, hydrolysis-resistant substrates such as lipids and lignin whose effective degradation requires O_2 (Emerson and Hedges, 1988; Canfield, 1994). The rate-determining step for both aerobic and anaerobic microbial degradation of polysaccharides and proteins is hydrolysis by extracellular enzymes, after which the released oligosaccharides and peptides less than ~600 amu are taken into cells for further alteration (Weiss *et al.*, 1991). Given this commonality and the fact that molecular oxygen is not required in the initial depolymerization phase, it is not surprising that these two major biochemical types often are both degraded effectively, although not necessarily at the same rates, under both oxic and anoxic conditions (Harvey *et al.*, 1995). In contrast, effective degradation of carbon-rich substrates and hydrolysis-resistant materials such as lignin, hydrocarbons, and pollen requires molecular oxygen, as opposed to simply water addition. Such degradation is often accomplished by O_2-requiring enzymes that catalyze electron (or hydrogen) removal or directly insert one or two oxygen atoms into organic molecules (Sawyer, 1991).

The most direct field evidence that the extent of sedimentary organic matter preservation is affected by exposure to bottom-water oxygen comes from oxidation fronts in deepsea turbidites of various ages and depositional settings (Wilson *et al.*, 1985; Weaver and Rothwell, 1987). One of these deposits in which the timing of the exposure to oxic and anoxic conditions is well documented, is the relict f-turbidite from the Madeira abyssal plain (MAP) ~700 km offshore of northwest Africa (Prahl *et al.*, 1989, 1997; Cowie *et al.*, 1995). This ~4 m-thick deposit was emplaced ~140 ka at a water depth of ~5,400 m when fine-grained carbonate-rich sediments slumped off the African continental slope and flowed down to cover the entire MAP with a texturally and compositionally uniform layer. This deposit was subsequently exposed to oxygenated bottom water for thousands of years during which time an oxidation front slowly penetrated approximately one-half meter into the turbidite before diffusive O_2 input was halted by accumulating sediment and the entire turbidite relaxed back to anoxic conditions (Buckley and Cranston, 1988). Pore-water sulfate concentrations measured within the sediments indicate little or no *in situ* sulfate reduction (De Lange *et al.*, 1987).

Comparative elemental analyses of the upper and lower sections of two sediment cores collected on the MAP show that organic concentrations decreased at both locations from values of 0.93–1.02 wt.% OC below the oxidation front to values 0.16–0.21 wt.% within the surface-oxidized layer (Figure 9). Pollen abundances decreased in the same samples from ~1,600 grains g^{-1} below the oxidation front to zero above it. Overall, 80% of the organic matter and essentially all of the pollen that has been stable for 140 kyr in the presence of pore-water sulfate was degraded in the upper section of the MAP cores as a result of long-term exposure to dissolved O_2.

The broad implication of these observations is that somewhere between upper continental margins and the deep ocean, depositional conditions lead to greatly increased exposure times of sedimentary organic matter to O_2 that are

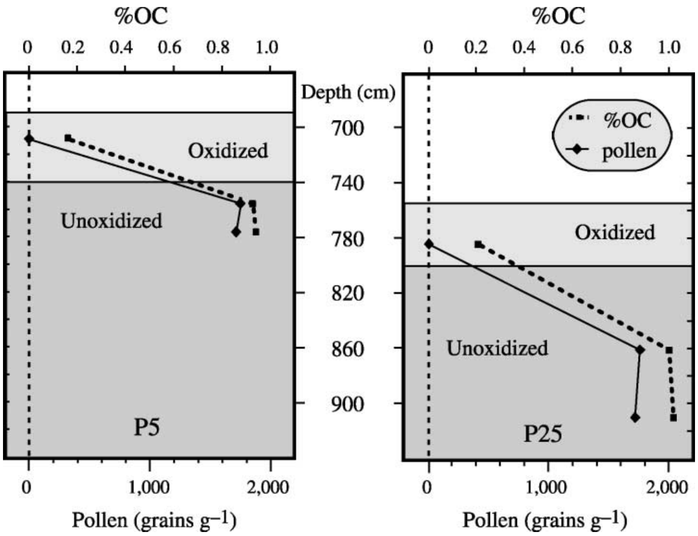

Figure 9 Profiles of the %OC and pollen abundances down two sequences of the f-turbidite from the MAP (source Cowie *et al.*, 1995) (reproduced by permission of Elsevier from *Geochim. Cosmochim. Acta* **1995**, *59*, 33–46).

sufficient to create the greatly reduced organic matter concentrations typical of modern-pelagic sediments (e.g., Figure 8). A test for this hypothesis was carried out for modern sediments depositing at varying distances and rates off the Washington State coast (see Hartnett *et al.*, 1998; Hedges *et al.*, 1999). Oxygen penetration depths were found to increase offshore from fractions of a centimeter in continental shelf and upper-slope sediments to over three centimeters in deeper (~3,000 m) offshore deposits. Average sediment accumulation rates decreased offshore from ~15 cm to 3 cm per thousand years. The combined result of these two trends is that oxygen exposure time (OET, the depth of oxygen penetration divided by the sedimentation rate) increases consistently offshore from decades on the continental shelf and upper slope to hundreds of years on the lower slope to over 1,000 yr at the most offshore study site. Corresponding concentrations of organic matter per unit sediment-surface area decreased consistently offshore from maximal values typical of upper-continental margin sediments depositing under oxygenated bottom water (~1 mg OC m^{-2}) to substantially lower concentrations (~0.3 mg OC m^{-2}) in offshore deep sediments. Mole percentages of nonprotein amino acids and physically corroded pollen increased consistently offshore, indicating that the remnant organic matter in deeper deposits is appreciably more degraded. Thus, over time spans of hundreds to thousands of years, exposure to molecular oxygen appears to affect both the amount and composition of organic matter preserved in continental margin sediments.

6.11.3 DIAGENESIS AND PRESERVATION OF CALCIUM CARBONATE

Between 20% and 30% of the carbonate produced in the surface ocean is preserved in marine sediments. The fraction of $CaCO_3$ produced that is buried dramatically affects the alkalinity and dissolved inorganic carbon (DIC) of seawater, and is thus important for understanding the processes that control the partial pressure of carbon dioxide in the atmosphere. Paleoceanographers have observed that the $CaCO_3$ content of marine sediments has changed with time in concert with glacial–interglacial periods. By studying the mechanisms that presently control $CaCO_3$ preservation, one seeks to understand what past changes imply about the chemistry of the ocean through time.

Sedimentary calcium carbonates are formed as the shells of marine plants and animals. Biologically produced $CaCO_3$ consists primarily of two minerals—aragonite and calcite. Shallow-water carbonates, primarily corals and shells of benthic algae (e.g., *Halimeda*) are heterogeneous in their mineralogy and chemical composition but are mainly composed of aragonite and magnesium-rich calcite (see Morse and Mackenzie (1990) for a discussion). Carbonate tests of microscopic plants and animals that live in the surface ocean (there are also benthic animals that produce carbonate shells) are primarily made of the mineral calcite, which composes the bulk of the $CaCO_3$ in deep-ocean sediments. A large fraction of the ocean floor consists of $CaCO_3$ from these tests (Figure 10). Note that the topographic rises on the ocean floor are $CaCO_3$-rich,

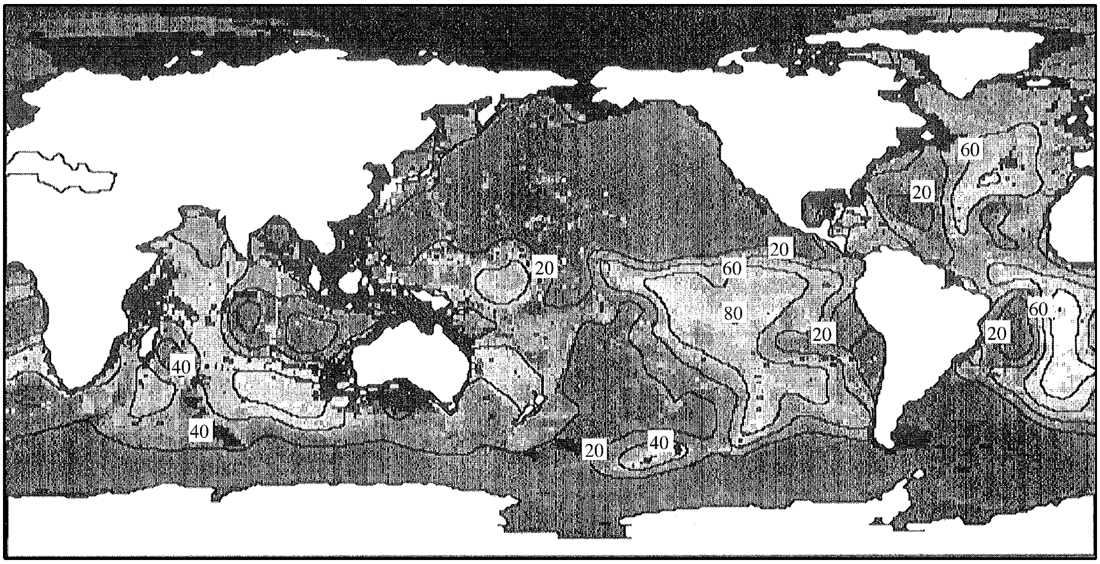

Figure 10 Global distribution of the wt.% $CaCO_3$ in surface sediments of the deep ocean (>1,000 m) (source Archer, 1996).

while the abyssal planes are barren of this mineral. The other noticeable major trend is that there is relatively little $CaCO_3$ in the sediments of the North Pacific. We focus next on the processes that control these distributions.

6.11.3.1 Mechanisms Controlling $CaCO_3$ Burial: Thermodynamics

The solubility of $CaCO_3$ in seawater has been studied extensively because of its great abundance in sedimentary rocks and the ocean. The equation for dissolution of pure calcium carbonate:

$$CaCO_{3(s)} \Leftrightarrow Ca^{2+} + CO_3^{2-} \tag{4}$$

has the simple "apparent" solubility product in seawater:

$$K'_{sp} = [Ca^{2+}][CO_3^{2-}] \tag{5}$$

The apparent constant, K'_{sp}, is related to thermodynamic constants, K_{sp}, via the total activity coefficients of Ca^{2+} and CO_3^{2-}. Apparent constants are usually used in seawater because laboratory determinations of the constants are determined in this medium.

The saturation state of seawater with respect to the solid is sometimes denoted by the Greek letter omega, Ω.

$$\Omega = [Ca^{2+}][CO_3^{2-}]/K'_{sp} \tag{6}$$

The numerator of the right side is the product of measured total concentrations of calcium and carbonate in the water—the ion concentration product (ICP). If $\Omega = 1$ then the system is in equilibrium and should be stable. If $\Omega > 1$, the waters are supersaturated, and the laws of thermodynamics would predict that the mineral should precipitate removing ions from solution until Ω returned to one. If $\Omega < 1$, the waters are undersaturated and the solid $CaCO_3$ should dissolve until the solution concentrations increase to the point where $\Omega = 1$. In practice it has been observed that $CaCO_3$ precipitation from supersaturated waters is rare probably because of the presence of the high concentrations of magnesium in seawater blocks nucleation sites on the surface of the mineral (e.g., Morse and Arvidson, 2002). Supersaturated conditions thus tend to persist. Dissolution of $CaCO_3$, however, does occur when $\Omega < 1$ and the rate is readily measurable in laboratory experiments and inferred from pore-water studies of marine sediments. Since calcium concentrations are nearly conservative in the ocean, varying by only a few percent, it is the apparent solubility product, K'_{sp}, and the carbonate ion concentration that largely determine the saturation state of the carbonate minerals.

The apparent solubility products of calcite and aragonite have been determined repeatedly in seawater solutions. We adopt the values of Mucci (1983) ($4.35(\pm 0.20) \times 10^{-7}$ and $6.65 (\pm 0.12) \times 10^{-7}$ $mol^2\,kg^{-2}$) for calcite and aragonite, respectively, at 25 °C, $S = 35$, and 1 atm pressure. These data agree within error with previous measurements of Morse *et al.* (1980) and represent many repetitions to give a clear estimate of the reproducibility ($\sim\pm 5\%$).

Because of the great depth of the ocean, the most important physical property determining the solubility of carbonate minerals in the sea is pressure. The pressure dependence of the equilibrium constants is related to the difference in volume, ΔV, occupied by the ions of Ca^{2+} and CO_3^{2-} in solution versus in the solid phase. The volume difference between the dissolved and solid phases is called the partial molal volume change, ΔV:

$$\Delta V = V_{Ca} + V_{CO_3} - V_{CaCO_3} \tag{7}$$

The change in partial molal volume for calcite dissolution is negative, meaning that the volume occupied by solid $CaCO_3$ is greater than the combined volume of the component Ca^{2+} and CO_3^{2-} in solution. Since with increasing pressure Ca^{2+} and CO_3^{2-} prefer the phase occupying the least volume, calcite becomes more soluble with pressure (depth) by a factor of ~2 for a depth increase of 4 km. Values of the partial molal volume change determined by laboratory experiments and *in situ* measurements result in a range of 35–45 $cm^3\,mol^{-1}$ (see Sayles, 1980; Millero and Berner, 1972; and Chapter 6.19). The uncertainty in this value is thus $\sim\pm 10\%$.

The final important factor affecting the solubility of $CaCO_3$ in the ocean is the concentration of carbonate ion. The high ratio of organic carbon to carbonate carbon in the particulate material degrading and dissolving in the deepsea causes the deep waters to become more acidic and carbonate poor as they progress along the conveyer belt circulation network from the North Atlantic to deep Indian and northern Pacific oceans. Carbonate ion concentrations change from ~250 $\mu mol\,kg^{-1}$ in surfaces waters to mean values in the deep waters of 113 $\mu mol\,kg^{-1}$ in the Atlantic, 83 in the Indian and South Pacific, and 70 $\mu mol\,kg^{-1}$ in the deep North Pacific oceans. There is little vertical difference in these values below 1,500 m (see Chapter 6.19). Thus the tendency for $CaCO_3$ minerals to be preserved is greatest in surface waters of the world's oceans and decreases "downstream" in deep waters from the Atlantic to Indian and Pacific oceans. The mean saturation horizon for calcite shoals from a depth of ~4.5 km in the equatorial Atlantic to 3.0 km in the Indian Ocean and South Pacific to less than 1.0 km in the North Pacific (Broecker and Peng, 1981; Feely *et al.*, 2003).

There have been many attempts to correlate the presence of calcite in marine sediments with

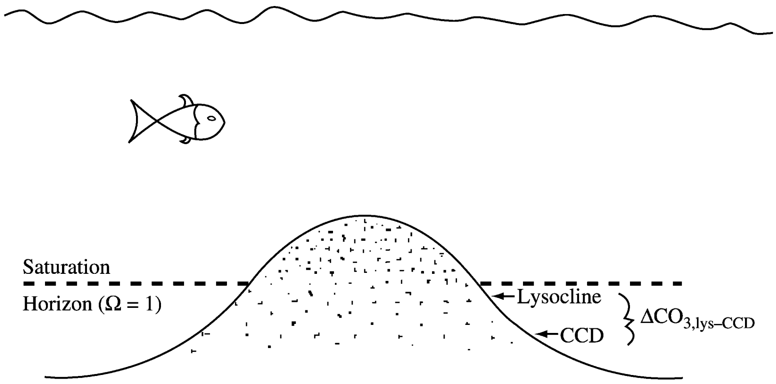

Figure 11 A sketch of the theoretical relationships among the depths of the lysocline, the CCD, and the saturation horizon ($\Omega = 1$). Dot density represents relative $CaCO_3$ content in the sediments.

the degree of saturation in the overlying water. The sketch in Figure 11 demonstrates the ideal relationship between the "saturation horizon" in the water (where $\Omega = 1$) and the presence of $CaCO_3$ in the sediments. The terminology for the presence of $CaCO_3$ in sediments is a little esoteric with the word "lysocline" coined to be the depth at which the first indication of dissolution of carbonates occurs and "carbonate compensation depth" (CCD) being the depth where the rain rate of calcium carbonate to the seafloor is exactly compensated by the rate of dissolution of $CaCO_3$ (i.e., where there is no longer burial of $CaCO_3$). It would seem that one could determine the importance of thermodynamics in determining calcite preservation by letting the ocean do the work and simply comparing lysocline and saturation-horizon relationships. There are two main problems with these attempts at direct observation. The first is the poor accuracy with which we know the degree of saturation in the ocean and the second is our inability to precisely determine the onset of $CaCO_3$ dissolution within sediments.

How well can we presently determine the saturation-horizon depth (where $\Omega = 1$) for calcite in the sea? If we assume that we know the calcium concentration exactly, then the error in Ω is determined by the errors in K'_{sp} and the measured carbonate ion concentration, $[CO_3^{2-}]$. Mucci (1983) was able to determine repeated laboratory measurements of the apparent solubility product, K'_{sp}, at 1 atm pressure to ~±5%, and the pressure dependence at 4 km is known to ~±10%. These errors compound to ±11% in the value of K'_{sp} (4 km). Carbonate ion concentrations in the sea are almost always calculated from A_T and DIC. Being slightly conservative about accuracy of these values in ocean surveys (±4 μeq kg^{-1} for A_T and ±2 μmol kg^{-1} for DIC; they can be determined with errors about half these values if conditions are perfect), and assuming we know exactly the value of the equilibrium constants in the carbonate system, the error in $[CO_3^{2-}]$ is ≈±4%. This uncertainty plus that for K'_{sp} compound the error in Ω to ±12%. Because $[CO_3^{2-}]$ values for the individual ocean basins are nearly vertical below 1.5 km, most of the change in Ω with depth is due to the pressure effect. The slope of K'_{sp} with depth at 4 km is equivalent to the change in saturation carbonate ion concentration, $[CO_3^{2-}]_{sat}$, with depth (~16 μmol km^{-1}; see Chapter 6.19). For the Atlantic Ocean where the $[CO_3^{2-}]$ below 1.5 km is ~110 μmol kg^{-1}, this represents a change of 14% km^{-1}. Thus, the uncertainty in the value of Ω is such that one does not know the saturation horizon in the ocean to better than ±0.90 km depth.

Determining the depth of the onset of dissolution from measurements of the $CaCO_3$ content of marine sediments involves nearly as much error. The reason is that the content of $CaCO_3$ in the sediments is insensitive to the fraction of $CaCO_3$ dissolved when the sediments are highly concentrated in $CaCO_3$. This is because the fraction dissolved is determined by flux balance, and measurements determine the percent carbonate in the sediment. For example, assume that the raining particulate material is 90 wt.% $CaCO_3$, with the remaining 10% being unreactive solids such as clay minerals. If there is no dissolution in the sediments then they also will be 90% $CaCO_3$. If half of the $CaCO_3$ dissolves, the sediments are still $4.5/(4.5 + 1) = 0.82$ or 82 wt.% $CaCO_3$. Thus, if we assume an error of ±5% in the $CaCO_3$ measurement, we would not be able to detect the onset of dissolution till about one-quarter of the raining material dissolved. There is often a very gradual change in the $CaCO_3$ concentration with depth at the top of the sedimentary transition zone or enough scatter in the data to cause determination of the depth of the onset of dissolution to have an error of at least ±0.5 km.

While errors in evaluating the depths of both the saturation horizon and the onset of $CaCO_3$ dissolution complicate "field" tests of the importance of chemical equilibrium, the difference in carbonate ion concentration over the depth range of the transition between calcite-rich and calcite-poor sediments is more clear because it is easier to know the difference in both $[CO_3^{2-}]$ and $CaCO_3$ wt.% than the absolute value. The difference, $\Delta CO_{3,\ \mathrm{lys-CCD}}$ ($= [CO_3^{2-}]_{\mathrm{lys}} - [CO_3^{2-}]_{\mathrm{CCD}}$; Figure 11), has been mapped by Archer (1996) in all areas of the ocean where both $[CO_3^{2-}]$ in the bottom water and $CaCO_3$ wt.% in sediments have been determined. The ocean mean is $19 \pm 12\ \mu\mathrm{mol\ kg^{-1}}$ ($n = 30$). The simple fact that the transition from $CaCO_3$-rich to $CaCO_3$-poor sediments occurs over a broad range of $[CO_3^{2-}]$ values indicates that the pattern of $CaCO_3$ preservation cannot be based on thermodynamics alone. Kinetic processes must be important.

6.11.3.2 Mechanism of $CaCO_3$ Dissolution: Kinetics

6.11.3.2.1 The dissolution rate constant

The dissolution rates of the minerals of calcium carbonate have been shown in laboratory experiments to follow the rate law:

$$R = k\{K'_{\mathrm{sp}} - \mathrm{ICP}\}^n \tag{8}$$

where k is the dissolution rate constant which has units necessary to match those of the rate. The exponent n is one for diffusion-controlled reactions and usually some higher number for surface-controlled reaction rates (see Morse and Arvidson, 2002). The above equation can be recast for $CaCO_3$ dissolution in two ways:

$$R = k\{[Ca^{2+}]_s[CO_3^{2-}]_s - [Ca^{2+}][CO_3^{2-}]\}^n \tag{9}$$

and, if $[Ca]_s = [Ca]$,

$$R = k[Ca^{2+}]^n\{[CO_3^{2-}] - [CO_3^{2-}]\}^n$$

where $k^* = k[Ca]^n$, alternatively,

$$R = k\{K'_{\mathrm{sp}}(1 - \Omega)\}^n = kK'^n_{\mathrm{sp}}(1 - \Omega)^n \tag{10}$$

where $k^* = kK'^n_{\mathrm{sp}}$.

These equations are indistinguishable for rate measurements at a single temperature and pressure, but predict different results for the variation of the rate constant, k^*, with environmental variables (i.e., T, P, and $[Ca^{2+}]$). Because $[Ca^{2+}]$ is not constant in laboratory experiments during the course of dissolution, Equation (10) is normally used to interpret these results (e.g., Morse and Arvidson, 2002; Keir, 1980). In the ocean, where $[Ca^{2+}]$ is nearly a constant but K'_{sp} varies dramatically with pressure, Equation (9) is more convenient.

There are several studies that have been successful in determining the dissolution rate at conditions near seawater saturation. Acker *et al.* (1987) was able to employ very precise determinations of pH to measure the rate of dissolution of a single pteropod shell at different pressures from 15 atm to 300 atm. Because his measurements were at different pressures and K'_{sp} is a function of pressure, he was able to determine whether the rate constant is indeed a function of K'_{sp}. He found that Equation (9) fit his data better than (10), suggesting that the constant is not pressure dependent and the former is a more accurate universal rate law. An exponent of $n = 1.9$ was obtained for this surface-controlled dissolution reaction and a partial molal volume, ΔV, of $-39\ \mathrm{cm^3\ mol^{-1}}$ (very close to the mean of the values determined in laboratory experiments for calcite) best fit the data.

The most extensive laboratory measurements of the dissolution of carbonates (Keir, 1980) employed a steady-state "chemostat" reactor to measure the dissolution rate of reagent grade calcite, coccoliths, foraminifera, synthetic aragonite, and pteropods. In these experiments the rate constant varied by a factor of ~100 between the different forms of calcite (after making the correction for surface area) and the data were interpreted with $n = 4.5$ order kinetics. While these measurements are still the standard for calcium carbonate dissolution rate kinetics, the high order kinetics have been reinterpreted (Hales and Emerson, 1997a) using more defendable K'_{sp} values to have a rate law that has an order of $n = 1-2$ (Figure 12). This result agrees much

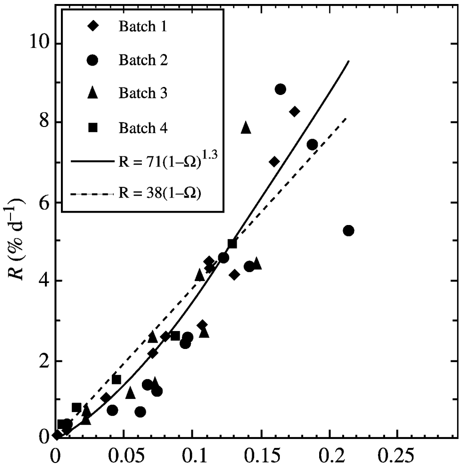

Figure 12 The dissolution rate (R in % $\mathrm{d^{-1}}$) for calcite from laboratory experiments of Keir (1980) as a function of the degree of undersaturation, $(1 - \Omega)$. Lines represent the rate laws with exponents of $n = 1.3$ and 1.0 (source Hales and Emerson, 1997a) (reproduced by permission of Elsevier from *Earth Planet. Sci. Lett.* **1997**, *148*, 317–327).

more closely with the aragonite experiments and dissolution rate laws determined for other minerals, and we adopt it as more likely than $n = 4.5$. Note that the units of the rate constant (Figure 12; $k = 0.38\ \mathrm{d}^{-1}$or 100 times this value, 38% d^{-1}) are normalized to the concentration of solid in the experimental reactor. A convenient way to view this rate constant is that the units represent moles $CO_3^{2-}\ \mathrm{cm}^{-3}\ \mathrm{d}^{-1}$ released to the water per mole of $CaCO_3\ \mathrm{cm}^{-3}$ in the solution, thus mol $\mathrm{cm}^{-3}\ \mathrm{d}^{-1}$/ mol $\mathrm{cm}^{-3} = \mathrm{d}^{-1}$. At the time of using the rate constant to calculate dissolution in the environment the units must be "transformed."

One of the great uncertainties in our understanding of the kinetics of $CaCO_3$ dissolution at this time is that the dissolution rate constants required to interpret ocean observations are much smaller than those measured in the laboratory. This can be illustrated rather simply by applying the observed laboratory kinetic rate constant to determine the ΔCO_3 necessary to produce the transition in $CaCO_3$ concentrations observed in marine sediments (Appendix A). To make the calculation we have to assume dissolution begins when the bottom waters become undersaturated with respect to calcite and then determine the flux of calcium from the sediments as the degree of undersaturation increases. It is assumed that the dissolution flux of $CaCO_3$ is equal to the flux of CO_3^{2-} from the sediments and that CO_3^{2-} does not react with other carbonate system ions in solution. These assumptions are, of course, incorrect but acceptable for a first order of approximation. (The 2 : 1 change in A_T and DIC, that accompanies $CaCO_3$ dissolution, increases the $[CO_3^{2-}]$ by ~35% of the DIC increase at pH = 7.5. Thus, the gradient of $[Ca^{2+}]$ would be ~3 times the gradient in $[CO_3^{2-}]$ at the pH of pore waters. This is considered an acceptable error for this demonstration.)

The result of the calculation (Appendix A) indicates that the rate constant necessary to create the $\Delta CO_{3,\mathrm{lys-CCD}} = 19\ \mu\mathrm{mol\ kg}^{-1}$, has to be at least 100 times less than the laboratory-determined values. This has been confirmed by *in situ* measurements (see later). Perhaps the most important lesson here is that models and laboratory experiments consider primarily pure phases whereas impurities and surface coatings may greatly influence dissolution rates in nature. Until there is better agreement between the laboratory and *in situ* model-determined values, the latter will have to be used in model reconstructions of the relationship between ocean chemistry and sedimentary carbonate content.

6.11.3.2.2 The effect of organic matter degradation

The relatively slow dissolution of calcite can explain the gradual change between carbonate-rich and carbonate-poor sediments. There is, however, another important issue that we have not considered—the role of organic matter degradation in sediments in promoting *in situ* calcite dissolution. It was long suspected that organic matter degradation would promote dissolution, but this was not quantified until the 1980s and 1990s. Two factors lead to the realization that the inorganic kinetic interpretation of $CaCO_3$ burial in the ocean was incomplete. First, observations of the carbon content of particles that rain to the ocean floor collected in sediment traps 1 km or less above the bottom suggest the molar organic carbon to $CaCO_3$ carbon rain ratio is about one. A few centimeters below the sediment surface this ratio is more like 0.1, indicating that something like 90% of the organic carbon that reaches the surface is degraded rather than buried. Second, sediment pore-water studies in the same areas as the sediment trap deployments show strong oxygen depletions in the top few centimeters. Simple-flux calculations require that the bulk of the organic matter degradation between the sinking particles and that buried takes place within the sediments (Emerson *et al.*, 1985; Figure 4). Thus, most particles that reach the seafloor are stirred into the sediments before they have a chance to degrade while sitting on the surface. If this were not the case, and the particles degraded on the surface, there would be little oxygen depletion within the sediments.

Organic matter degradation within the sediments creates a microenvironment that is corrosive to $CaCO_3$ even if the bottom waters are not, because addition of DIC and no A_T to the pore water causes it to have a lower pH and smaller $[CO_3^{2-}]$. Using a simple analytical model and first-order dissolution rate kinetics, Emerson and Bender (1981) predicted that this effect should result in up to 50% of the $CaCO_3$ that rains to the seafloor being dissolved even at the saturation horizon, where the bottom waters are saturated with respect to calcite. Because the percent $CaCO_3$ in sediments is so insensitive to dissolution and the saturation-horizon depth so uncertain, this suggestion was well within the constraints of environmental observations.

The effect of organic matter driven dissolution is to raise the carbonate transition in sediments relative to the saturation horizon in the water column (Emerson and Archer, 1990; Figure 11), but there should be little change in the $\Delta CO_{3,\mathrm{lys-CCD}}$ necessary to create the transition in $\%CaCO_3$. Thus, the argument about the relationship between the dissolution rate constant and observed transition of $\%CaCO_3$ in sediments (Appendix A) should not be affected.

The suggestion of "organic $CaCO_3$ dissolution" in sediments has been tested by determining the gradient of oxygen and $[CO_3^{2-}]$ in the sediment pore waters. This had to be done on a very fine (millimeter) scale because the important region for the reaction is near the sediment–water interface. The test required *in situ* measurements because it has been shown the pH values of pore waters change when they are depressurized. To do this Archer *et al.* (1989) and later Hales and Emerson (1996) built an instrument capable of traveling to the deepsea sediment surface, slowly inserting oxygen and pH microelectrodes, one millimeter at a time, into the sediments and recording the data *in situ*. The results of these experiments, some of which are reproduced in Figure 13, confirmed the prediction that a significant amount of $CaCO_3$ dissolves because of organic matter degradation. The pH of the pore waters cannot be interpreted without assuming dissolution of $CaCO_3$ in response to organic matter degradation measured by the pore-water oxygen profiles. This process makes the burial of $CaCO_3$ in the ocean dependent not only on thermodynamics and kinetics but also on the particulate rain ratio of organic carbon to calcium carbonate carbon. The kinetic rate constant required to model the measured pH profiles (Figure 13) is more than 2 orders of magnitude smaller than that measured in laboratory experiments which is consistent with the simple argument presented earlier in Appendix A.

There has always been some reluctance to assume that the pH in a porous medium is controlled solely by the carbonate buffer system in the pore waters. There are arguments that H^+ ions on particle surfaces can affect pH measurements (Stumm and Morgan, 1981) and, even more importantly, comprehensive models of pore-water chemistry are beginning to demonstrate that H^+ adsorption on mineral surfaces may play an important role in controlling the pH of pore waters. Conclusions of the pH measurements, however, have been confirmed by millimeter-scale measurements of both p_{CO_2} and calcium concentration in the pore waters (Hales *et al.*, 1997; Cai *et al.*, 1995; Wenzhofer *et al.*, 2001.)

Observations from benthic-flux experiments in which A_T and calcium fluxes have been measured both below and above the calcite saturation horizon confirm the effect of organic matter degradation on the dissolution of $CaCO_3$ in most (e.g., Berelson *et al.*, 1990; Jahnke *et al.*, 1997) but not all situations. R. J. Jahnke and D. B. Jahnke (2002) interpret their benthic-flux measurements at five locations in the world's ocean to show that in regions with sediments of very high $CaCO_3$ content there appears to be no evidence of metabolic dissolution of $CaCO_3$ based on A_T and calcium benthic fluxes. They suggest that the reason for this observation is that the pH of pore waters is controlled by adsorption of hydrogen ion and carbonate species on the surface of $CaCO_3$. Transport of these species to and from the sediment surface by bioturbation creates a flux that is more important than that caused by molecular diffusion in the pore waters.

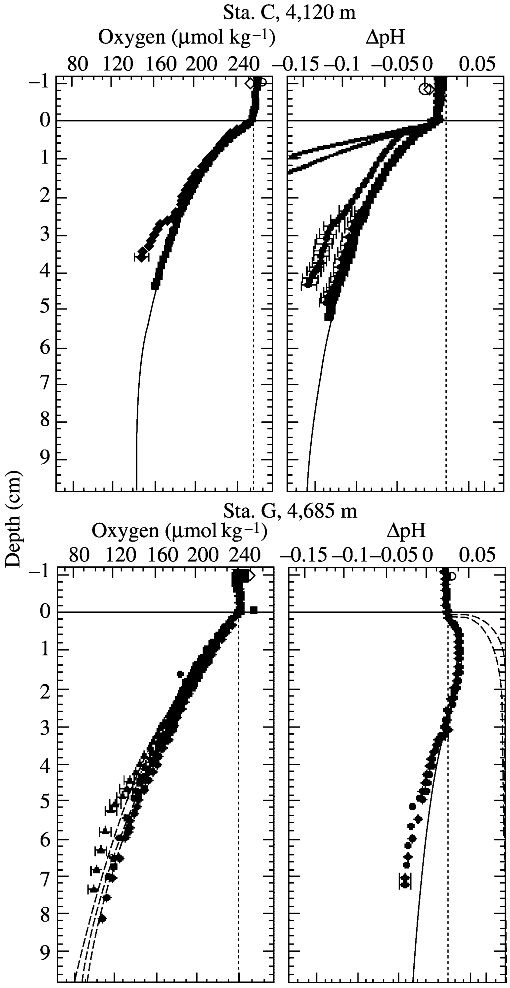

Figure 13 Pore-water profiles of oxygen concentration and ΔpH (The pH difference between the value in the pore water and the value in bottom water) in the top ~10 cm of sediments from two locations on the Ceara Rise. Points are individual measurements, sometimes from different electrodes on the same deployment. Open symbols in the overlying water are measurements in the bottom water after the pore-water profile. Solid and dashed curves are model solutions. In the top figure (Sta. C) the bottom waters are saturated with respect to calcite. The thick solid lines on the top right figure indicate the predicted ΔpH if there were no $CaCO_3$ dissolution caused by organic matter degradation in the sediments. In the bottom figure (Sta. G) bottom waters are undersaturated with respect to calcite. The dashed lines in the right figure indicate the trend if there were only dissolution promoted by bottom-water undersaturation (after Hales and Emerson, 1997b) (reproduced by permission of Elsevier from *Geochim. Cosmochim. Acta* **1997**, *61*, 501–514).

Potential problems with this interpretation are that it stems from very small changes in the chambers of the benthic landers, because open ocean areas high in $CaCO_3$ are locations with relatively low organic matter degradation rates. In addition, the surface properties of $CaCO_3$ in seawater have not been measured sufficiently well to incorporate adsorption effects into diagenesis models. The observations, however, demand interpretation, and, if adsorption effects turn out to be important, it will have ramifications for interpreting mechanisms of $CaCO_3$ preservation because of the wide-spread distribution of $CaCO_3$-rich sediments.

Recent measurements of calcium and alkalinity in the ocean above the calcite saturation horizon (Milliman *et al.*, 1999; Chen, 2002) suggest dissolution in supersaturated waters. The proposed mechanisms are variations of the organic matter driven $CaCO_3$ dissolution mechanism. In these cases the authors suggest that microenvironments in falling particulate material (Milliman *et al.*, 1999) or anerobic dissolution in sediments of the continental shelves and marginal seas (Chen, 2002) are locations of $CaCO_3$ dissolution. As the details and accuracy of measurements improve, thermodynamic and kinetic mechanisms required to interpret the results become more and more complex.

6.11.3.2.3 The interpretation of the ^{14}C age of surface sediments

Determining the ^{14}C accumulation rate as a function of the degree of saturation should be a sensitive way of determining the extent and mechanism of $CaCO_3$ dissolution in sediments. The ^{14}C age of the bioturbated layer (the top 4–8 cm of sediments based on the constancy of ^{14}C measurements) and the accumulation rate below depend on the rain rate and dissolution flux of $CaCO_3$. Two simple end-member cases illustrate the complexity of interpreting core top ^{14}C data. If dissolution takes place within the sediments, as it must for organic matter-driven dissolution to be effective, and all $CaCO_3$ particles dissolve at the same rate, the radiocarbon age should decrease with the extent of dissolution—the reservoir size decreases but the influx remains the same. In this case the probability of survival of all $CaCO_3$ particles is the same so there would be fewer older particles in the sediment mixed layer with more intense dissolution. If, however, dissolution takes place primarily at the sediment–water interface before the particles are mixed into the sediment, or for some reason younger particles dissolve faster, the mixed layer ages would increase with progressive dissolution because the input flux decreases faster than the reservoir size.

Broecker *et al.* (1999 and references therein) argued, based on bioturbated layer sediment ^{14}C-$CaCO_3$ measurements, that increase in age with depth in the western equatorial Pacific is either due to interface or non-steady-state dissolution. This would argue against the importance of organic matter driven dissolution. DuBois and Prell (1988), however, present data that indicate the ^{14}C age of the sediment bioturbated layer on the Sierra Leone Rise in the eastern equatorial Atlantic decreases as dissolution increases with greater depth (Figure 14) suggesting that homogeneous dissolution dominates. Keir and Michel (1993) concluded that these simple end-member calculations are complicated by a non-steady-state increase in dissolution during the Holocene.

While there appear to be a variety of interpretations of the origin of core-top ^{14}C data, recent measurements of pore-water ^{14}C (Martin *et al.*, 2000) have helped to identify the age of the $CaCO_3$ particles undergoing dissolution. Pore-water $DI^{14}C$ measurements are sensitive to the mechanism of dissolution because dissolved $DI^{14}C$ changes due to calcite dissolution directly reflect the age of the dissolving particles. An age for the added ^{14}C that is similar to the age of the mixed layer (4,000 yr or so) indicates homogeneous dissolution is most important; a much younger age indicates interface dissolution is more important. The other advantage of this method is that it traces processes that have occurred relatively recently. The timescale for replacement of the top-ten centimeters of

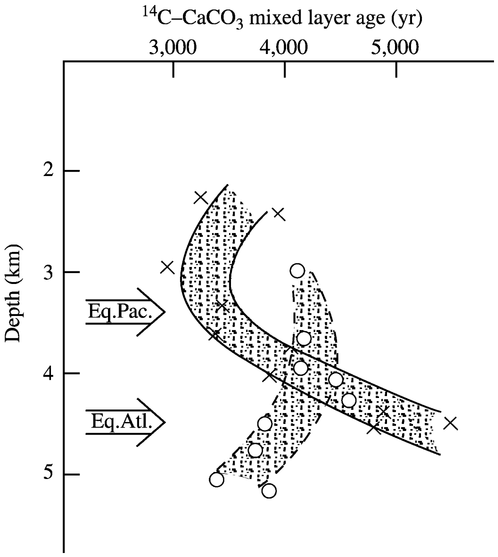

Figure 14 The ^{14}C-$CaCO_3$ age of the sediment bioturbated layer as a function of water depth on the Ontong–Java Plateau (X) in the western equatorial Pacific (Broecker *et al.*, 1999) and the Sierra Leone Rise (O) in the eastern equatorial Atlantic (DuBois and Prell, 1988). The arrows indicate the depth of the first signs of $CaCO_3$ dissolution in the sediments as based on $\%CaCO_3$ (for the Pacific) and $\%CaCO_3$ fragments (for the Atlantic).

pore-water DIC by diffusion is years rather than thousands of years for the processes that control sediment ages. Martin *et al.* (2000) measured pore-water DI^{14}C at a stations above and below the saturation horizon in the western equatorial Pacific. Below the saturation horizon, where $CaCO_3$ dissolves spontaneously by inorganic processes, DI^{14}C values indicate younger particles are preferentially dissolved, in accordance with the sediment ^{14}C ages that increase with greater undersaturation and interface dissolution. Pore-water DIC from the sediments above the saturation horizon, however, had ages that are more consistent with a mixture of interface particles undergoing homogeneous dissolution.

It appears at the time of writing this chapter that the mechanisms determining the ^{14}C age of surface sediments are variable and may be different for different saturation states even at the same ocean location. This observation, compounded by the non-steady-state possibility (Keir and Michel, 1993) indicates that the mechanisms controlling core top ^{14}C ages are probably too complicated to distinguish the importance of organic matter driven dissolution.

6.11.4 DIAGENESIS AND PRESERVATION OF SILICA

Biogenic silica, in the form of opal, makes up an important part of marine sediments, particularly in the southern and eastern equatorial oceans (Figure 15). These deposits are formed primarily from tests of diatoms that lived in the surface oceans. More than half of the opal formed in the surface ocean is dissolved within the upper 100 m and only a small percentage of the production is ultimately buried in marine sediments (Nelson *et al.*, 1995). Rewards to be gained by understanding the mechanisms that control opal diagenesis in sediments are evaluating the utility of the SiO_2 concentration changes in sediments as a tracer for past diatom production and understanding the role of authigenic silicates as a sink for major ions in marine geochemical mass balances.

The main tool for studying diagenesis and preservation of SiO_2 in marine sediments has been the measurement of H_4SiO_4 in pore waters which has occurred since the 1970s (e.g., the early work of Hurd (1973) and Fanning and Pilson (1974); Figure 16). The difficulty in interpreting these results has been that the asymptotic values in pore-water profiles, the concentration that is achieved by 10 cm below the sediment–water interface, is highly variable geographically where solid opal is preserved in the sediments. Possible explanations for these observations fall into three general categories (McManus *et al.*, 1995). First, asymptotic values may be different because the solubility of opal formed in surface waters varies geographically. Second, pore waters may never achieve equilibrium but opal formed in surface waters has a number of phases of different reactivity which, in concert with sediment bioturbation, create different steady-state asymptotic values. Finally, diagenesis reactions within the sediments may create authigenic phases other than opal that control the pore-water solubility and chemical kinetics of H_4SiO_4.

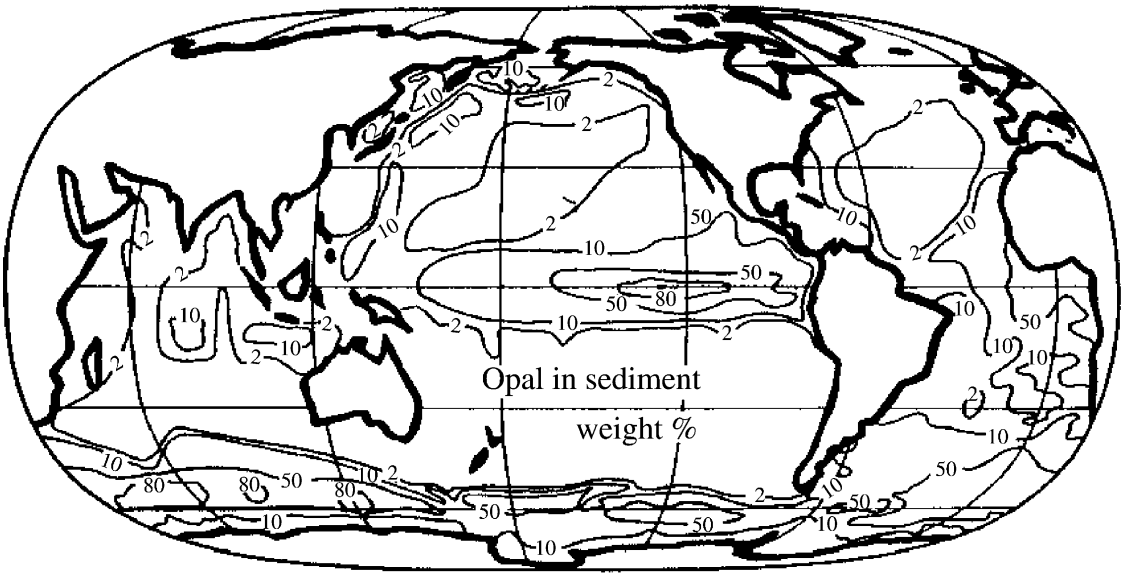

Figure 15 The global distribution of SiO_2 in marine sediments in weight percent (after Broecker and Peng, 1982).

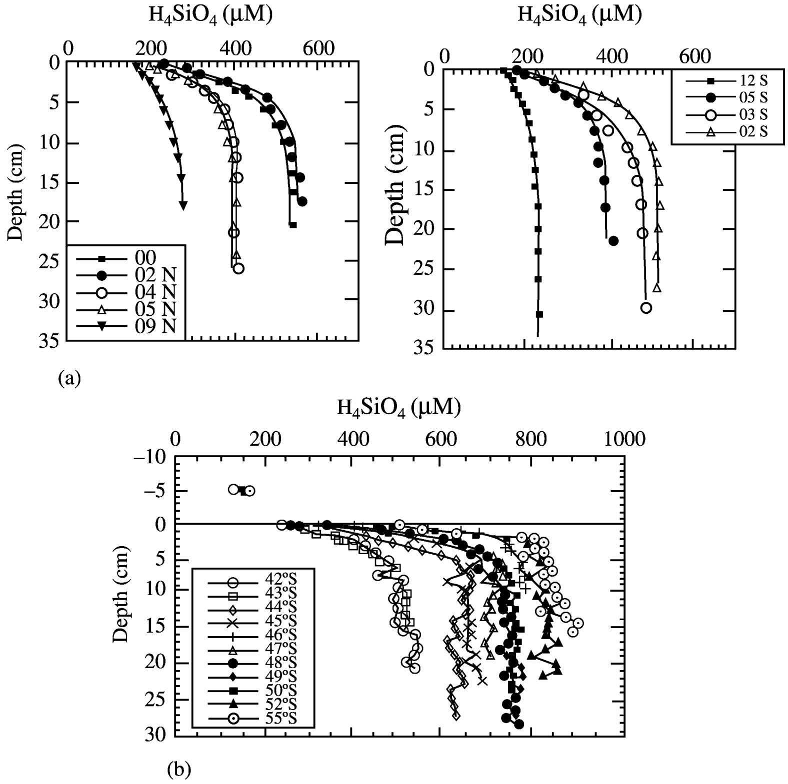

Figure 16 Pore-water H_4SiO_4 concentrations as a function of depth in sediment on (a) a North–South transect along 140° W in the equatorial Pacific (after McManus *et al.*, 1995) (reproduced by permission of Elsevier from *Deep-Sea Res. II* **1995**, *42*, 871–902) and (b) a North–South transect through the Indian sector of the Polar Front (after Rabouille *et al.*, 1997) (reproduced by permission of Elsevier from *Deep-Sea Res. II* **1997**, *44*, 1151–1176).

6.11.4.1 Controls on the H_4SiO_4 Concentration in Sediment Pore Waters: Thermodynamics

Even before the wide variety of asymptotic pore-water values in marine sediments were observed, it was shown (e.g., Hurd, 1973; Lawson *et al.*, 1978) that the H_4SiO_4 concentration obtained by incubating diatom frustrules obtained from surface waters was greater than that observed in pore waters. The equilibrium solubility is much too high to explain the results, and equilibrium values for other SiO_2 minerals are even higher. More recent experiments in sediments from the Southern Ocean using stirred flow-through reactors indicate saturation concentrations that range between 1,000 mol L^{-1} H_4SiO_4 and 1,600 mol L^{-1} H_4SiO_4 (Van Cappellen and Qiu, 1997a), values that are much greater than those determined in the pore-water profiles from the same location (Figure 16). These results lend little support to the hypothesis that the asymptotic values are equilibrium concentrations of different opals produced in the surface waters. However, we shall see later that thermodynamics does play a role in explaining the observations.

6.11.4.2 Controls on the H_4SiO_4 Concentration in Sediment Pore Waters: Kinetics

Early studies of the rate of opal dissolution in the laboratory indicated that the dissolution rate of acid-cleaned planktonic diatoms varied as a linear function of the degree of undersaturation (e.g., Hurd, 1973; Lawson *et al.*, 1978).

$$d[H_4SiO_4]/dt = k_{Si}S\{[H_4SiO_4]_{sat} - [H_4SiO_4]\} \quad (11)$$

where k_{Si} is the rate constant for SiO_2 dissolution (cm s^{-1}) and S is the solid surface area (cm^2 cm^{-3}). Generally, the dissolution rate constants determined by these methods are much greater than those needed to model the pore-water profiles, indicating some important differences between the laboratory experiments and field results, just as in the case for $CaCO_3$ dissolution kinetics.

The first attempt to use the dynamics of dissolution and burial in marine sediments to explain the pore-water observations was the elegant interpretation by Schink *et al.* (1975). They assumed opal fractions of different reactivity—one that dissolves rapidly and completely and another that is essentially refractory. The idea was that the first fraction, in concert with sediment bioturbation, sets the pore-water asymptotic concentration of H_4SiO_4 and the refractory portion determines the sediment concentration of opal. The reason that bioturbation is important in defining the pore-water concentration of H_4SiO_4 is that it stirs the opal deeper into the sediments where dissolution is more effective in creating a strong concentration gradient.

One can illustrate the relationships among bioturbation, dissolution kinetics and the asymptotic concentration in sediment pore waters rather simply in the following way. If we assume that the reactive portion of the opal rain to the sediment–water interface dissolves in the top *h* cm of the sediments, then the residence times for the reactive opal concentration, $[SiO_2]_{sed}$ (mol cm_s^{-3}), with respect to *in situ* dissolution is:

$$\tau_{diss} = h(1-\varphi)f[SiO_2]_{sed}/F_{Si} \qquad (12)$$

where φ is the porosity ($cm_{pw}^3\,cm_b^{-3}$), f is the fraction of the sediment that is opal and F_{Si} (mol $cm^{-2}\,s^{-1}$) is the flux of H_4SiO_4 to the overlying water. Since all the reactive opal dissolves, this residence time is roughly equal to the mean time required to stir opal, by bioturbation, to the depth, h:

$$\tau_{trub} = h^2/2D_b \qquad (13)$$

where D_b is the bioturbation coefficient ($cm^2\,s^{-1}$). If we assume that a simple steady-state balance between diffusion and dissolution controls the distribution of H_4SiO_4 (mol cm_{pw}^{-3}) in sediment pore waters, then:

$$D_{Si}\frac{d^2[H_4SiO_4]}{dz^2} = -kS\{[H_4SiO_4]_{asy} - [H_4SiO_4]\} \qquad (14)$$

where D_{Si} is the molecular diffusion coefficient of silicic acid ($cm^2\,s^{-1}$), and kS is the kinetic rate constant (s^{-1}). The boundary condition at $z=0$ constrains the surface concentration to be that of the bottom water, $[H_4SiO_4]_{BW}$, and the value at depth when $z \rightarrow \infty$, approaches $[H_4SiO_4]_{asy}$, the asymptotic concentration. This relationship is exactly analogous to the diffusion–reaction equation for CO_3^{2-} (Appendix A; Equation (20)) and the flux at the sediment–water interface is

$$F_{Si} = (kSD_{Si})^{0.5}\Delta H_4SiO_4 \qquad (15)$$

where $\Delta H_4SiO_4 = \{[H_4SiO_4]_{asy} - [H_4SiO_4]_{BW}\}$. Substituting this value for the flux in Equation (12) and equating the two residence-time equations gives:

$$\Delta H_4SiO_4 = \{2(1-\varphi)f[SiO_2]/h(kSD_{Si})^{0.5}\}D_b \qquad (16)$$

The asymptotic concentration is proportional to the value of the bioturbation coefficient. Observed values for the terms on the right of the above equation indicate that these approximations reproduce measured pore-water values adequately given the crudeness of the model (Appendix B).

While the dynamics of this interpretation are instructive for realizing the importance of bioturbation, explaining the field observations by this mechanism requires changes in the bioturbation coefficient over short distances that have not been measured and provides no explanation for the refractory portion of the opal flux.

Van Cappellen and Qiu (1997b) used flow-through reactor studies to demonstrate that the dissolution rate of unaltered silicon-rich sediment from the Southern Ocean follows a rate law that is exponential rather than linear with respect to the degree of undersaturation. The implication is that the rate of dissolution is much greater near the sediment–water interface than below. In fact they find that, when the laboratory kinetic studies are applied to the sediments, SiO_2 dissolution is pretty much finished below a few centimeters. Rabouille *et al.* (1997) and McManus *et al.* (1995) interpreted pore-water H_4SiO_4 profiles (Figure 16) using a model that incorporated a depth-dependent rate constant.

The question remains as to what processes cause the kinetics of opal dissolution to change as the mineral ages in marine sediments. A striking clue to the answer was the observation that the asymptotic H_4SiO_4 pore-water values in Southern Ocean sediments are strongly dependent on the amount of detrital material present in the opal-rich sediments (Figure 17). Since earlier studies had established that aluminum is reactive in marine sediments (Mackin and Aller, 1984), this correlation implies that detrital aluminosilicates supply the aluminum necessary for reactions that take place very soon after deposition.

6.11.4.3 The Importance of Aluminum and the Rebirth of "Reverse Weathering"

Field observations implicating the importance of aluminosilicates to opal diagenesis were followed by laboratory experiments to determine the effect of Al(III) derived from detrital aluminum silicate on the solubility and dissolution kinetics of opal. Dixit *et al.* (2001) mixed opal-rich (~90% SiO_2) sediments from the Southern Ocean with different amounts of either kaolinite or ground basalt in long-term (21 months) batch

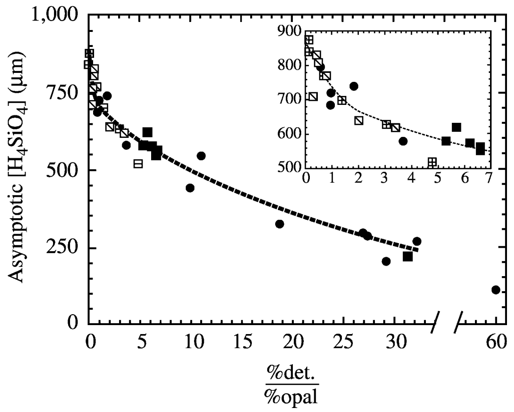

Figure 17 The relationship between the asymptotic H_4SiO_4 concentration in pore waters and the relative detrital and opal content of the sediments (Van Cappellen, personal communication). (Data from (●) Rickert (2000); (⊠) King *et al.* (2000); (■) Koning *et al.* (1997); (⊞) Van Cappellen and Qiu (1997a)).

experiments. The observed concentration of H_4SiO_4 at the end of these experiments was strongly influenced by the presence of the aluminosilicate phase. Values ranged from ~1,000 μmol kg^{-1} H_4SiO_4 for nearly pure opal to ~400 μmol kg^{-1} for a 1 : 4 aluminosilicate : opal mixture. An authigenic phase forms in the presence of dissolved silicon and aluminum that is less soluble than pure opal. They found that the pore-water aluminum concentration and the Al : Si ratio of diatom frustrules in surface sediments were also proportional to the amount of detrital material in the sediments. The substitution of Al(III) for one in 70 of the silicon atoms in opal decreased its solubility by ~25%.

The depression in opal solubility with incorporation of aluminum clarifies many aspects of the field observations but not all. Equilibrium arguments alone cannot explain why pore waters in sediments with high concentrations of detrital material are observed to remain undersaturated with respect to the experimentally determined opal solubility. Kinetic experiments using flow-through reactors (Dixit *et al.*, 2001) revealed that active precipitation of authigenic aluminosilicates prevented the pore waters from reaching equilibrium with the opal phase present in the sediments. Also, studies of the surface chemistry of biogenic silicates (Dixit and Van Cappellen, 2002) indicate that changes in the surface chemical structure during diagenesis contributes to slower kinetics. Thus, the laboratory studies indicate the mechanisms that explain model interpretations of pore-water H_4SiO_4 concentrations are surface chemical changes and authigenic aluminosilicate formation. Precipitation of authigenic aluminosilicate minerals must be one of the most widespread diagenesis reactions occurring in marine sediments.

While these reactions presently imply only the substitution of aluminum for silicon, this mechanism, and field observations of the geochemistry of aluminum in tropical near-shore sediments (e.g., Mackin and Aller, 1984), bring us back to authigenic process suggested by Mackenzie and Garrels (1966) to close the marine geochemical imbalance for Mg^{2+}, K^+, and HCO_3^- created during weathering on land. The generalized scheme for the proposed "reverse weathering" reaction was

$$\begin{aligned}&H_4SiO_4 + \text{degraded clay from land} + HCO_3^-\\&\quad + Mg^{2+},\ K^+ \rightarrow \text{ion-rich authigenic clay}\\&\quad + CO_2 + H_2O\end{aligned}$$

The popularity of this proposal waned owing to lack of strong evidence to prove that it occurred, and fluxes suggested in the early studies of hydrothermal processes (Edmond *et al.*, 1979) obviated the need for low-temperature reactions to balance the river inflow of Mg^{2+} and HCO_3^-. This has changed since we now know that the flow of water through high-temperature zones of hydrothermal areas is less than previously suggested, and the importance of low-temperature reactions and flows are uncertain.

The quantitative importance of "reverse weathering" reactions were demonstrated by the rapid formation of authigenic aluminosilicates in the sediments of the Amazon delta (Michalopoulos and Aller, 1995). These authors placed seed materials (glass beads, quartz grains, and quartz grains coated with iron oxide) into anoxic Amazon delta sediments. After 12–36 months they observed the formation of K–Fe–Mg-rich clay minerals on the seed materials and suggest that formation of these materials in Amazon sediments alone could account for removal of 10% of the global riverine input of K^+. Since environments like the Amazon delta account for ~60% of the flux of detrital material to the oceans, the impact of these reactions globally might be much greater than in this delta alone.

Both the tropical "reverse weathering" studies and the recent discovery of the process controlling opal diagenesis in surface sediments demonstrate the importance of rapid authigenic aluminosilicate formation in marine sediments. The focus is now back on determining the importance of these reactions in marine geochemical mass balances. The role of detrital material in the preservation of opal complicates the utility of SiO_2 as a paleoceanographic tracer. This role will depend on understanding whether there is a proportionality between opal flux to sediments and the preservation rate.

APPENDIX A

Approximating the role of calcite dissolution kinetics in determining the width of the $CaCO_3$ transition from 90% to 10% in marine sediments

(i) *The carbon-flux balance at the sediment–water interface.* The $CaCO_3$ rain rate to the sediment–water interface, R_{Ca} is assigned to be 1.5 g_{CaCO_3} m^{-2} yr^{-1} and the burial rate, B_{Ca}, is calculated from Equation (17) for different values of the dissolution flux, F_{Ca}.

$$R_{Ca} = B_{Ca} + F_{Ca}(\text{mol cm}^{-2}\text{s}^{-1}) \qquad (17)$$

(ii) *Derivation of the $CaCO_3$ dissolution flux, F_{Ca}, as a function of the degree of carbonate saturation from CO_3 dynamics at the sediment–water interface.*

Assume $F_{Ca} = F_{CO_3}$, and as a first order of approximation, ignore all carbonate equilibrium reactions in the solution (see text). In this case the steady-state diffusion–reaction equation for CO_3 concentration, $[CO_3^{2-}]$ (mol cm^{-3}), in the pore waters is

$$0 = D\{d^2\varphi[CO_3]/dz^2\} - \varphi J'(\text{mol cm}^{-3}\,\text{s}^{-1}) \qquad (18)$$

where z is depth in the pore waters, φ is porosity, and D (cm^2 s^{-1}) is the molecular diffusion coefficient for CO_3^{2-}. Assuming first-order kinetics, the dissolution rate is given by

$$J' = k'\{[CO_3] - [CO_3]_s\} \qquad (19)$$

where $[CO_3]_s$ is the carbonate concentration in equilibrium with calcite, and, k' (s^{-1}) is the *in situ* dissolution rate constant. If porosity is not a function of z, $[CO_3] = [CO_3]^0$ at $z = 0$, and $[CO_3]$ approaches $[CO_3]_{sat}$ as $z \rightarrow \infty$, the flux at the sediment–water interface, $z = 0$ is

$$\begin{aligned} F_{CO_3} &= -\varphi D\{d[CO_3]/dz\}_{z=0} \\ &= \phi(Dk')^{1/2}\{[CO_3]_0 - [CO_3]_s\} \qquad (20) \end{aligned}$$

Table 4 shows the relationship between the degree of undersaturation, ΔCO_3, and the fraction of $CaCO_3$ in sediments, f, for different values of the dissolution rate constant, k. The results are based on the mass balance model described below.

(iii) *The relationship between $CaCO_3$ rain, burial, and the fraction of $CaCO_3$ in sediments* (R_D and B_D = detrital rain rate and burial rate, mol cm^{-2} s^{-1}).

Above the lysocline, where there is no $CaCO_3$ dissolution:

$$R_{Ca}/(R_{Ca} + R_D) = f_0 \qquad (21)$$

Below the lysocline:

$$B_{Ca}/(B_{Ca} + B_D) = f \qquad (22)$$

Since $R_D = B_D$:

$$f = B_{Ca}/\{(R_{Ca}/f_0) - R_{Ca} + B_{Ca}\} \qquad (23)$$

(iv) The values of the fraction of $CaCO_3$, f, preserved in the sediments as a function of the degree of undersaturation, ΔCO_3, calculated from Equations (17), (20), and (23) for three different rate constants are shown in Table 4.

Laboratory dissolution rate constants, k, were transferred to values used in Equation (19), k', by multiplying the lab rate equation, $j = k(1 - \Omega)$, by the concentration of $CaCO_3$ in sediments, $[CaCO_3]$, (J' in Equation (19) $= J[CaCO_3]$)

$$J[CaCO_3] = k[CaCO_3]\ (1 - \Omega)$$

To change from $(1 - \Omega)$ to $\{[CO_3^{2-}]_s - [CO_3^{2-}]\}$ multiply by $K'_{sp}/[Ca^{2+}]$:

$$\begin{aligned} &K'_{sp}/[Ca^{2+}](1 - [Ca^{2+}][CO_3^{2-}]/K'_{sp}) \\ &\quad = ([CO_3^{2-}]_s - [CO_3^{2-}]) \end{aligned}$$

Thus,

$$\begin{aligned} J[CaCO_3] = &- k[CaCO_3]\{[Ca^{2+}]/K'_{sp}\}([CO_3^{2-}] \\ &- [CO_3^{2-}]_s) \end{aligned}$$

and

$$k' = k[CaCO_3]([Ca^{2+}]/K'_{sp})$$

Table 4

ΔCO_3 (mol cm^{-3} × 10^{-9})	F_{Ca}[a] (mol m^{-2} s^{-2} × 10^{13})			B_{Ca}[b] (mol m^{-2} s^{-2} × 10^{13})			f[c]		
	$k =$ 0.38 d^{-1}	$k =$ 0.038 d^{-1}	$k =$ 0.0038 d^{-1}	$k =$ 0.38 d^{-1}	$k =$ 0.038 d^{-1}	$k =$ 0.0038 d^{-1}	$k =$ 0.38 d^{-1}	$k =$ 0.038 d^{-1}	$k =$ 0.0038 d^{-1}
0	0	0	0	4.7	4.7	4.7	0.90	0.90	0.90
5	10.6	3.3	1.0		1.4	3.7	0	0.73	0.88
10	21.6	6.7	2.1			2.6	0	0	0.83
20	42.2	13.3	4.2			0.3	0	0	0.36

[a] Equation (20) with $D_{CO_3} = 1 \times 10^{-6}$ cm^2 s^{-1}, $\varphi = 0.9$ and k the three cases in $k = 0.38$ d^{-1}, 0.038 d^{-1}, and 0.0038 d^{-1}. [b] Equation (17) with $R_{Ca} = 4.7 \times 10^{-13}$ mol m^{-2} s^{-1} (1.5 g_{CaCO_3} cm^{-2} kyr^{-1}). [c] Equation (23) with $f_0 = 0.9$.

Evaluating $[\mathrm{CaCO_3}]$ and $[\mathrm{Ca^{2+}}]/K'_{\mathrm{sp}}$

$$[\mathrm{CaCO_3}] = f(1-\varphi)\rho/M = 0.5(0.1)2.5/100$$
$$= 1.25\times10^{-3}\ \mathrm{mol_{CaCO_3}\ cm_{bulk}^{-1}}$$

$$[\mathrm{Ca^{2+}}]/K'_{\mathrm{sp}} = 0.01\ \mathrm{mol\ cm^{-3}}/10^{-12}\ \mathrm{mol^2\ cm^{-6}}$$
$$(\text{at 4 km})$$
$$= 10^7(\mathrm{mol^{-1}\ cm^3})$$

APPENDIX B

Importance of bioturbation to the asymptotic concentration of H_4SiO_4 in marine sediment pore waters

We consider the simple balance presented in Equation (16):

$$\Delta\mathrm{H_4SiO_4} = \{2(1-\varphi)f[\mathrm{SiO_2}]/h(kSD)^{0.5}\}D_\mathrm{b}$$

where:

- $f = 0.5$ is the fraction of opal in the sediments;
- $(1-\varphi) = 0.3$ ($\mathrm{cm_s^3\ cm_b^{-3}}$), porosity, $\varphi = 0.7$;
- $[\mathrm{SiO_2}] = \rho/M = 2.0\ \mathrm{g\ cm_s^{-3}}/65\ \mathrm{g_{SiO_2}\ mol^{-1}} = 0.031\ \mathrm{mol\ cm_s^{-3}}$;
- $h = 5$ cm, the $1/e$ depth of the pore-water profiles (Figure 16);
- $kS = 1\times10^{-7}\ \mathrm{s^{-1}}$ (2 °C) from pore-water models (Broecker and Peng, 1982; Hurd, 1973; Vanderborght *et al.*, 1977); $D_{\mathrm{H_4SiO_4}}$ (2 °C) $= 2\times10^{-6}$.

Values of D_B in the equatorial Pacific Ocean are $(7-40)\times10^{-9}\ \mathrm{cm^2\ s^{-1}}$ from ^{210}Pb and ^{234}Th profiles, respectively (McManus *et al.*, 1995):

D_b ($\mathrm{cm^2\ s^{-1}}$)	$[\mathrm{H_4SiO_4}]_{\mathrm{asy}} - [\mathrm{H_4SiO_4}]_{\mathrm{BW}}$ (μmol $\mathrm{L^{-1}}$)
10^{-9}	4
10^{-8}	42
10^{-7}	416

REFERENCES

Acker J. G., Byre R. H., Ben-Yaakov S., Feely R. A., and Betzer P. R. (1987) The effect of pressure on aragonite dissolution rates in seawater. *Geochim. Cosmochim. Acta* **51**, 2171–2175.

Aller R. C. (1982) The effects of macrobenthos on chemical properties of marine sediment and overlying water. In *Animal-sediment Relations* (eds. D. L. McCall and M. J. S. Tevesz). Plenum, New York, pp. 53–102.

Aller R. C. (1984) The importance of relict burrow structures and burrow irrigation in controlling sedimentary solute distributions. *Geochim. Cosmochim. Acta* **48**, 1929–1934.

Aller R. C. (1990) Bioturbation and manganese cycling in hemipelagic sediments. *Phil. Trans. Roy. Soc. London A* **331**, 51–68.

Aller R. C., Mackin J. E., and Cox R. T. (1986) Diagenesis of Fe and S in Amazon inner shelf muds: apparent dominance of Fe reduction and implications for the genesis of ironstones. *Continent. Shelf Res.* **6**, 263–389.

Archer D. (1996) An atlas of the distribution of calcium carbonate in sediments of the deep sea. *Global Biogeochem. Cycles* **10**, 159–174.

Archer D. and Devol A. (1992) Benthic oxygen fluxes on the Washington shelf and slope: a comparison of *in situ* microelectrode and chamber flux measurements. *Limnol. Oceanogr.* **37**, 614–629.

Archer D., Emerson S. R., and Reimers C. E. (1989) Dissolution of calcite in deep-sea sediments: pH and O_2 microelectrode results. *Geochim. Cosmochim. Acta* **53**, 2831–2845.

Archer D. E., Morford J. L., and Emerson S. (2002) A model of suboxic sedimentary diagenesis suitable for automatic tuning and gridded global domains. *Global Biogeochem. Cycles* **16** (1), doi 10.1029/2000G001288.

Atlas R. M., Boehm P. D., and Calder J. A. (1981) Chemical and biological weathering of oil from the Amoco Cadiz spillage within the littoral zone. *Estuar. Coast. Shelf Sci.* **12**, 589–608.

Bender M. L. (1990) The δ^{18}O of dissolved O_2 in seawater: a unique tracer of circulation and respiration in the deep sea. *J. Geophys. Res.* **95**, 22243–22252.

Bender M. L., Fanning K., Froelich P. N., Heath G. R., and Maynard V. (1977) Interstitial nitrate profiles and oxidation of sedimentary organic matter in the eastern equatorial Atlantic. *Science* **198**, 605–609.

Benner R., Maccubbin A. E., and Hodson R. E. (1984) Anaerobic biodegradation of the lignin and polysaccharide components of lignocellulose and synthetic lignin by sediment microflora. *Appl. Environ. Microbiol.* **47**, 998–1004.

Berelson W. M., Hammond D., and Cutter G. A. (1990) *In situ* measurements of calcium carbonate dissolution rates in deep-sea sediments. *Geochim. Cosmochim. Acta* **54**, 3013–3020.

Bergamaschi B. A., Tsamakis E., Keil R. G., Eglinton T. I., Montluçon D. B., and Hedges J. I. (1997) The effect of grain size and surface area on organic matter, lignin and carbohydrate concentration, and molecular compositions in Peru margin sediments. *Geochim. Cosmochim. Acta* **61**, 1247–1260.

Berner R. A. (1974) Kinetic models for the early diagenesis of nitrogen, sulfur, phosphorus, and silicon in anoxic marine sediments. In *The Sea* (ed. E. D. Goldberg). Wiley, New York, vol. 5, pp. 427–450.

Berner R. A. (1980) *Early Diagenesis: A Theoretical Approach*. Princeton University Press, Princeton, NJ.

Berner R. A. (1989) Biogeochemical cycles of carbon and sulfur and their effect on atmospheric oxygen over phanerozoic time. *Palaeogeogr. Palaeoclimatol. Palaeoecol.* **73**, 97–122.

Boudreau B. P. (1984) On the equivalence of non-local and radial diffusion models for pore water irrigation. *J. Mar. Res.* **42**, 731–735.

Boudreau B. P. (1997) *Diagenetic Models and their Implication: Modeling Transport and Reactions in Aquatic Sediments*. Springer, Berlin.

Boudreau B. P. and Ruddick B. R. (1991) On a reactive continuum representation of organic matter diagenesis. *Am. J. Sci.* **291**, 507–538.

Brandes J. A. and Devol A. H. (1997) Isotopic fractionation of oxygen and nitrogen in coastal marine sediments. *Geochim. Cosmochim. Acta* **61**, 1793–1801.

Broecker W. S. and Peng T.-H. (1982) *Tracers in the Sea*. Lamont-Doherty Geological Observatory, Palisades, NY.

Broecker W. S., Clark E., McCorkle D. C., Hajdas I., and Bonani G. (1999) Core top ^{14}C ages as a function of latitude and water depth on the Ontong-Java plateau. *Paleoceanography* **14**, 13–22.

Buckley D. E. and Cranston R. E. (1988) Early diagenesis in deep sea turbidites: the imprint of paleo-oxidation zones. *Geochim. Cosmochim. Acta* **52**, 2925–2939.

Cai W.-J., Reimers C. E., and Shaw T. (1995) Microelectrode studies of organic carbon degradation and calcite dissolution at a California continental rise site. *Geochim. Cosmochim. Acta* **59**, 497–511.

Calvert S. E. and Pedersen T. F. (1992) Organic carbon accumulation and preservation in marine sediments: how important is anoxia? In *Organic Matter* (eds. J. Whelan and J. W. Farrington). University Press, New York, pp. 231–263.

Canfield D. E. (1994) Factors influencing organic carbon preservation in marine sediments. *Chem. Geol.* **114**, 315–329.

Canfield D. E., Thamdrup B., and Hansen J. W. (1993) The anaerobic degradation of organic matter in Danish coastal sediments: iron reduction, manganese reduction and sulfate reduction. *Geochim. Cosmochim. Acta* **57**, 3867–3883.

Chen C.-T. A. (2002) Shelf vs. dissolution-generated alkalinity above the chemical lysocline. *Deep-Sea Res. II* **49**, 5365–5375.

Christensen J. P., Devol A. H., and Smethie W. M. (1984) Biological enhancement of solute exchange between sediments and bottom water on the Washington continental shelf. *Continent. Shelf Res.* **3**, 9–23.

Cowie G. L., Hedges J. I., Prahl F. G., and De Lange G. J. (1995) Elemental and major biochemical changes across an oxidation front in a relict turbidite: a clear-cut oxygen effect. *Geochim. Cosmochim. Acta* **59**, 33–46.

De Lange G. J., Jarvis I., and Kuijpers A. (1987) Geochemical characteristics and provenance of late quaternary sediments from the Madeira abyssal plains N. Atlantic. In *Geology and Geochemistry of Abyssal Plains* (eds. P. P. E. Weaver and J. Thomson). Blackwell, London, pp. 147–165.

Dixit S. and Van Cappellen P. (2002) Surface chemistry and reactivity of biogenic silica. *Geochim. Cosmochim. Acta* **66**, 2559–2568.

Dixit S., Van Cappellen P., and van Bennekom A. J. (2001) Process controlling solubility of biogenic silica and pore water build-up of silicic acid in marine sediments. *Mar. Chem.* **73**, 333–352.

DuBois L. G. and Prell W. L. (1988) Effects of carbonate dissolution on the radiocarbon age structure of sediment mixed layers. *Deep-Sea Res.* **35**, 1875–1885.

Edmond J. M., *et al.* (1979) Ridge crest hydrothermal activity and the balances of the major and minor elements in the ocean: the galapagos data. *Earth Planet. Sci. Lett.* **46**, 1–18.

Emerson S. R. and Archer D. (1990) Calcium carbonate preservation in the ocean. *Phil. Trans. Roy. Soc. London A* **331**, 29–40.

Emerson S. R. and Bender M. I. (1981) Carbon fluxes at the sediment–water interface of the deep-sea: calcium carbonate preservation. *J. Mar. Res.* **39**, 139–162.

Emerson S. and Hedges J. I. (1988) Processes controlling the organic carbon content of open ocean sediments. *Paleoceanography* **3**, 621–634.

Emerson S., Fisher K., Reimers C., and Heggie D. (1985) Organic carbon dynamics and preservation in deep-sea sediments. *Deep-Sea Res.* **32**, 1–21.

Emerson S., Jahnke R., and Heggie D. (1984) Sediment–water exchange in shallow water estuarine sediments. *J. Mar. Res.* **42**, 709–730.

Fanning K. A. and Pilson M. E. Q. (1974) Diffusion of dissolved silica out of deep-sea sediments. *J. Geophys. Res.* **79**, 1293–1297.

Feely R. A., Sabine C. L., Lee K., Millero F. J., Lamb M. F., Greeley D., Bullister J. L., Key R. M., Peng T.-H., Kozyr A., Ono T., and Wong C. S. (2002) *In-situ* calcium carbonate dissolution in the Pacific Ocean. *Global Biogeochem. Cycles* **16** (4), 1144, doi 10.1029/2002GB001866.

Froelich P. N., Klinkhammer G. P., Bender M. L., Ludtke N. A., Heath G. R., Cullin D., Dauphin P., Hammond D., Hartman B., and Maynard V. (1979) Early oxidation of organic matter in pelagic sediments of the eastern equatorial Atlantic: suboxic diagenesis. *Geochim. Cosmochim. Acta*, 1075–1090.

Grundmanis V. and Murray J. W. (1982) Aerobic respiration in pelagic marine sediments. *Geochim. Cosmochim. Acta* **46**, 1101–1120.

Hales B. and Emerson S. R. (1996) Calcite dissolution in sediments of the Ontong-Java plateau: *in situ* measurements of pore water O_2 and pH. *Global Biogeochem. Cycles* **10**, 527–541.

Hales B. and Emerson S. R. (1997a) Evidence in support of first-order dissolution kinetics of calcite in seawater. *Earth Planet. Sci. Lett.* **148**, 317–327.

Hales B. and Emerson S. R. (1997b) Calcite dissolution in sediments of the Ceara rise: *in situ* measurements of pore water O_2, pH, and CO_2(aq). *Geochim. Cosmochim. Acta* **61**, 501–514.

Hales B., Burgess L., and Emerson S. (1997) An absorbance-based fiber-optic sensor for CO_2(aq) measurements in pore waters of seafloor sediments. *Mar. Chem.* **59**, 51–62.

Hartnett H. E., Keil R. G., Hedges J. I., and Devol A. H. (1998) Influence of oxygen exposure time on organic carbon preservation in continental margin sediments. *Nature* **391**, 572–574.

Harvey H. R., Tuttl J. H., and Bell J. T. (1995) Kinetics of phytoplankton decay during simulated sedimentation: changes in biochemical composition and microbial activity under oxic and anoxic conditions. *Geochim. Cosmochim. Acta* **59**, 3367–3377.

Hedges J. I. and Keil R. G. (1995) Sedimentary organic matter preservation: an assessment and speculative synthesis. *Mar. Chem.* **49**, 81–115.

Hedges J. I., Cowie G. L., Ertel J. R., Barbour R. J., and Hatcher P. G. (1985) Degradation of carbohydrates and lignins in buried woods. *Geochim. Cosmochim. Acta.* **49**, 701–711.

Hedges J. I., Hu F. S., Devol A. H., Hartnett H. E., and Keil R. G. (1999) Sedimentary organic matter preservation: a test for selective oxic degradation. *Am. J. Sci.* **299**, 529–555.

Hurd D. C. (1973) Interactions of biogenic opal sediment and seawater in the central equatorial Pacific. *Geochim. Cosmochim. Acta* **37**, 2257–2282.

Imboden D. M. (1975) Interstitial transport of solutes in non-steady state accumulating and compacting sediments. *Earth Planet. Sci. Lett.* **27**, 221–228.

Jahnke R. A. (1996) The global ocean flux of particulate organic carbon: a real distribution and magnitude. *Global Biogeochem. Cycles* **10**, 71–88.

Jahnke R. J. and Jahnke D. B. (2002) Calcium carbonate dissolution in deep-sea sediments: implications of bottom water saturation state and sediment composition. *Geochim. Cosmochim. Acta* (in press).

Jahnke R. J., Craven D. B., McCorkle D. C., and Reimers C. E. (1997) $CaCO_3$ dissolution in California continental margin sediments: the influence of organic matter remineralization. *Geochim. Cosmochim. Acta* **61**, 3587–3604.

Jørgensen B. B. (1979) A comparison of methods for the quantification of bacterial sulfate reduction in coastal marine sediments: II. Calculation from mathematical models. *Geomicrobiol. J.* **1**, 29–47.

Keil R. G., Tsamakis E., Fuh C. B., Giddings J. C., and Hedges J. I. (1994a) Mineralogical and textural controls on organic composition of coastal marine sediments: hydrodynamic separation using SPLITT fractionation. *Geochim. Cosmochim. Acta.* **57**, 879–893.

Keil R. G., Montluçon D. B., Prahl F. G., and Hedges J. I. (1994b) Sorptive preservation of labile organic matter in marine sediments. *Nature* **370**, 549–552.

Keir R. S. (1980) The dissolution kinetics of biogenic calcium carbonates in seawater. *Geochim. Cosmochim. Acta* **44**, 241–252.

Keir R. S. and Michel R. L. (1993) Interface dissolution control of the ^{14}C profile in marine sediment. *Geochim. Cosmochim. Acta* **57**, 3563–3573.

King S. L., Froelich P. N., and Jahnke R. A. (2000) Early diagenesis of germanium in sediments of the Antarctic South Atlantic: in Search of the missing Ge-sink. *Geochim. Cosmochim. Acta* **64**, 1375–1390.

Koning E., Brummer G.-J., van Raaphorst W., van Bennekom J., Helder W., and van Iperen J. (1997) Settling dissolution and burial of biogenic silica in the sediments off Somalia (northwestern Indian Ocean). *Deep-Sea Res. II* **44**, 1341–1360.

Kristensen E. and Holmer M. (2001) Decomposition of plant materials in marine sediment exposed to different electron acceptors (O_2, NO_3^-, and SO_4^{2-}), with emphasis on substrate origin, degradation kinetics, and the role of bioturbation. *Geochim. Cosmochim. Acta* **65**, 419–433.

Lawson D. S., Hurd D. C., and Pankratz H. S. (1978) Silica dissolution rates of decomposing assemblages at various temperatures. *Am. J. Sci.* **278**, 1373–1393.

Lee C. (1992) Controls on organic carbon preservation: the use of stratified water bodies to compare intrinsic rates of decomposition in oxic and anoxic systems. *Geochim. Cosmochim. Acta* **56**, 3323–3335.

Mackenzie F. T. and Garrels R. M. (1966) Chemical mass balance between rivers and oceans. *Am. J. Sci.* **264**, 507–525.

Mackin J. E. and Aller R. C. (1984) Dissolved Al in sediments and waters of the East China Sea: implications for authigenic mineral formation. *Geochim. Cosmochim. Acta* **48**, 281–297.

Martin W. R., McNichol A. P., and McCorkle D. C. (2000) The radiocarbon age of calcite dissolving at the sea floor: estimates from pore water data. *Geochim. Cosmochim. Acta* **64**, 1391–1404.

Martins C., Kipphut G. W., and Klump J. V. (1980) Sediment–water chemical exchange in the coastal zone traced by *in situ* radon-222 flux measurements. *Science* **208**, 285–288.

Mayer L. M. (1994a) Surface area control of organic carbon accumulation in continental shelf sediments. *Geochim. Cosmochim. Acta* **58**, 1271–1284.

Mayer L. M. (1994b) Relationships between mineral surfaces and organic carbon concentrations in soils and sediments. *Chem. Geol.* **114**, 347–363.

Mayer L. M. (1999) Extent of coverage of mineral surfaces by organic matter in marine sediments. *Geochim. Cosmochim. Acta* **63**, 207–215.

McManus J., Hammond D. E., Berelson W. M., Kilgore T. E., DeMaster D. J., Ragueneau O. G., and Collier R. W. (1995) Early diagenesis of biogenic opal: dissolution rates, kinetics, and paleoceanographic implications. *Deep-Sea Res. II* **42**, 871–902.

Michalopoulos P. and Aller R. C. (1995) Rapid clay mineral formation in the Amazon delta sediments: reverse weathering and ocean elemental cycles. *Science* **270**, 614–617.

Middelburg J. J. (1989) A simple rate model for organic matter decomposition in marine sediments. *Geochim. Cosmochim. Acta* **53**, 1577–1581.

Middelburg J. J., Soetaert K., Herman P. M. J., and Heip C. H. R. (1996) Denitrification in marine sediments: a model study. *Global Biogeochem. Cycles* **10**, 661–673.

Millero F. J. and Berner R. A. (1972) Effect of pressure on carbonate equilibria in seawater. *Geochim. Cosmochim. Acta* **36**, 92–98.

Milliman J. D., Troy P. J., Balch W. M., Adams A. K., Li Y. H., and Mackenzie F. T. (1999) Biologically mediated dissolution of calcium carbonate above the chemical lysocline? *Deep-Sea Res. I* **46**, 1653–1669.

Morford J. and Emerson S. (1999) The geochemistry of redox sensitive trace metals in sediments. *Geochim. Cosmochim. Acta* **63**, 1735–1750.

Morse J. W. and Arvidson R. S. (2002) The dissolution kinetics of major sedimentary carbonate minerals. *Earth Sci. Rev.* **58**, 51–84.

Morse J. W. and Mackenzie F. T. (1990) *Geochemistry of Sedimentary Carbonates*. Elsevier, New York, NY.

Morse J. W., Mucci A., and Millero F. J. (1980) The solubility of calcite and aragonite in seawater at 35 ppt salinity at 25°C and atmospheric pressure. *Geochim. Cosmochim. Acta* **44**, 85–94.

Mucci A. (1983) The solubility of calcite and aragonite in seawater at various salinities, temperatures, and one atmosphere total pressure. *Am. J. Sci.* **283**, 780–799.

Murray J. W. and Kuivila K. M. (1990) Organic matter diagenesis in the northeast Pacific: transition from aerobic red clay to suboxic hemipelagic sediments. *Deep-Sea Res.* **37**, 59–80.

Murray J. W., Grundmanis V., and Smethie W. (1978) Interstitial water chemistry in the sediments of Saanich Inlet. *Geochim. Cosmochim. Acta* **42**, 1011–1026.

Nelson D. M., Treguer P., Brzezinski M. A., Leynaert A., and Queguiner B. (1995) Production and dissolution of biogenic silica in the ocean: revised global estimates, comparison with regional data and relationship to biogenic sedimentation. *Global Biogeochem. Cycles* **9**, 359–372.

Nittrouer C. A., *et al.* (1991) Sedimentology and stratigraphy of the Amazon continental shelf. *Oceanography* **4**, 33–38.

Pedersen T. F. and Calvert S. E. (1990) Anoxia vs. productivity: what controls the formation of organic-carbon-rich sediments and sedimentary rocks? *Am. Assoc. Petrol. Geol. Bull.* **74**, 454–466.

Prahl F. G., De Lange G. J., Lyle M., and Sparrow M. A. (1989) Post-depositional stability of long-chain alkenones under contrasting redox conditions. *Nature* **341**, 434–437.

Prahl F. P., De Lang G. J., Scholten S., and Cowie G. L. (1997) A case of post-depositional aerobic degradation of terrestrial organic matter in turbidite deposits from the Madeira abyssal plain. *Org. Geochem.* **27**, 141–152.

Premuzic E. T., Benkovitz C. M., Gaffney J. S., and Walsh J. J. (1982) The nature and distribution of organic matter in the surface sediments of world oceans and seas. *Org. Geochem.* **4**, 63–77.

Rabouille C., Gaillard J.-F., Treguer P., and Vincendeau M.-A. (1997) Biogenic silica recycling in surficial sediments across the Polar front of the Southern Ocean (Indian sector). *Deep-Sea Res. II* **44**, 1151–1176.

Raiswell R., Canfield D. E., and Berner R. A. (1994) A comparison of iron extraction methods for the determination of the degree of pyritization and the recognition of iron-limited pyrite formation. *Chem. Geol.* **111**, 101–110.

Ransom B., Bennett R. H., Baerwald R., and Shea K. (1997) TEM study of "*in situ*" organic matter on continental margins: occurrence and the "monolayer" hypothesis. *Mar. Geol.* **138**, 1–9.

Ransom B., Ki D., Kastner M., and Wainright S. (1998) Organic matter preservation on continental slopes: importance of mineralogy and surface area. *Geochim. Cosmochim. Acta* **62**, 1329–1345.

Reeburgh W. S. (1980) Anaerobic methane oxidation: rate depth distribution in Skan Bay sediments. *Earth Planet. Sci. Lett.* **47**, 345–352.

Rickert D. (2000) Dissolution kinetics of biogenic silica in marine environments. PhD Thesis, Ber. Polarforsch., 351.

Rutgers van der Loeff M. M. (1990) Oxygen in pore waters of deep-sea sediments. *Phil. Trans. Roy. Soc. London A* **331**, 69–84.

Sawyer D. T. (1991) *Oxygen Chemistry*. Oxford Press, New York.

Sayles F. L. (1980) The solubility of $CaCO_3$ in seawater at 2°C based upon *in-situ* sampled pore water composition. *Mar. Chem.* **9**, 223–235.

Sayles F. L., Martin W. R., and Deuser W. G. (1994) Response of benthic oxygen demand to particulate organic carbon supply in the deep sea near Bermuda. *Nature* **371**, 686–689.

Schink D. R., Guinasso N. L., and Fanning K. A. (1975) Processes affecting the concentration of silica at the sediment–water interface of the Atlantic Ocean. *J. Geophys. Res.* **80**, 2013–3031.

Sillen L. G. (1961) The physical chemistry of sea water. In *Oceanography*, Am. Assoc. Adv. Sci. Pub. 67 (ed. M. Sears). Washington, DC, pp. 549–581.

Smith C. R. and Rabouille C. (2002) What controls the mixed-layer depth in deep-sea sediments? The importance of POC flux. *Limnol. Oceanogr.* **47**, 418–426.

Smith C. R., Pope R. H., DeMaster D. J., and Magaard L. (1993) Age-dependent mixing of deep-sea sediments. *Geochim. Cosmochim. Acta* **57**, 1473–1488.

Smith K. L. and Baldwin R. J. (1984) Seasonal fluctuations in deep-sea sediment community oxygen consumption: central and eastern North Pacific. *Nature* **307**, 624–626.

Stumm W. and Morgan J. J. (1981) *Aquatic Chemistry*. Wiley, New York, NY.

Suess E. (1973) Interaction of organic compounds with calcium carbonate: II. Organo-carbonate association in recent sediments. *Geochim. Cosmochim. Acta* **37**, 2435–2447.

Sun M.-Y., Lee C., and Aller R. C. (1993a) Laboratory studies of oxic and anoxic degradation of chlorophyll-a in long island sound sediments. *Geochim. Cosmochim. Acta* **57**, 147–157.

Sun M.-Y., Lee C., and Aller R. C. (1993b) Anoxic and oxic degradation of ^{14}C-labeled chloropigments and a ^{14}C-labeled diatom in long island sound sediments. *Limnol. Oceanogr.* **38**, 1438–1451.

Tromp T. K., Van Cappellen P., and Key R. M. (1995) A global model for the early diagenesis of organic carbon and organic phosphorus in marine sediments. *Geochim. Cosmochim. Acta* **59**, 1259–1284.

Van Cappellen P. and Qiu L. (1997a) Biogenic silica dissolution in sediments of the Southern Ocean: I. Solubility. *Deep-Sea Res. II* **44**, 1109–1128.

Van Cappellen P. and Qiu L. (1997b) Biogenic silica dissolution in sediments of the Southern Ocean: I. Kinetics. *Deep-Sea Res. II* **44**, 1129–1149.

Vanderborght J. P., Wollast R., and Billen B. (1977) Kinetic model of diagenesis in disturbed sediments: mass transfer properties and silica diagenesis. *Limnol. Oceanogr.* **33**, 787–793.

Wang Y. and Van Cappellen P. (1996) A multicomponent reactive transport model of early diagenesis: application to redox cycling in coastal marine sediments. *Geochim Cosmochim. Acta* **60**, 2993-3014 .

Weaver P. P. E. and Rothwell R. G. (1987) Sedimentation on the Madeira abyssal plain over the last 300,000 years. In *Geology and Geochemistry of Abyssal Plains* (eds. P. P. E. Weaver and J. Thomson). Blackwell, London, pp. 71–86.

Weiss M. S., Abele U., Weckesser J., Welte W., Schultz E., and Schultz G. E. (1991) Molecular architecture and electrostatic properties of a bacterial porin. *Science* **254**, 1627–1630.

Wenzhofer F., Adler M., Kohls O., Hensen C., Strotmann B., Boehme S., and Schulz H. D. (2001) Calcite dissolution driven by benthic mineralization in the deep sea: *in situ* measurements of Ca^{2+}, pH, pCO_2 and O_2. *Geochim. Cosmochim. Acta* **65**, 2677–2690.

Westrich J. T. and Berner R. A. (1984) The role of sedimentary organic matter in bacterial sulfate reduction: the G model tested. *Limnol. Oceanogr.* **29**, 236–249.

Wilson T. R. S., Thomson J., Colley S., Hydes D. J., Higgs N. C., and Sørensen J. (1985) Early organic diagenesis: the significance of progressive subsurface oxidation fronts in pelagic sediments. *Geochim. Cosmochim. Acta* **49**, 811–822.

Treatise on Geochemistry
ISBN (set): 0-08-043751-6
Volume 6; (ISBN: 0-08-044341-9); pp. 293–319